Award Number: W81XWH-12-1-0613

TITLE: HOXC9-Induced Differentiation in Neuroblastoma Development

PRINCIPAL INVESTIGATOR: Han-fei Ding, Ph.D.

CONTRACTING ORGANIZATION: Georgia Health Sciences University Research Institute, Inc.

Augusta, GA 30912

REPORT DATE: October 2013

TYPE OF REPORT: Annual

PREPARED FOR: U.S. Army Medical Research and Materiel Command
Fort Detrick, Maryland 21702-5012

REPORT DOCUMENTATION PAGE

Form Approved
OMB No. 0704-0188

1. REPORT DATE *(DD-MM-YYYY)*	2. REPORT TYPE	3. DATES COVERED *(From - To)*
October 2013	Annual	09/30/2012 – 09/29/2013

4. TITLE AND SUBTITLE
HOXC9-Induced Differentiation in Neuroblastoma Development

5a. CONTRACT NUMBER

5b. GRANT NUMBER
W81XWH-12-1-0613

5c. PROGRAM ELEMENT NUMBER

6. AUTHOR(S)
Han-fei Ding, Ph.D.
hding@gru.edu

5d. PROJECT NUMBER

5e. TASK NUMBER

5f. WORK UNIT NUMBER

7. PERFORMING ORGANIZATION NAME(S) AND ADDRESS(ES)
Georgia Health Sciences University Research Institute, Inc
1120 15th Street
Augusta, GA 30912-4810

8. PERFORMING ORGANIZATION REPORT NUMBER

9. SPONSORING / MONITORING AGENCY NAME(S) AND ADDRESS(ES)
USA MED RESEARCH MAT CMD

FORT DETRICK MD 21702-5012

10. SPONSOR/MONITOR'S ACRONYM(S)

11. SPONSOR/MONITOR'S REPORT NUMBER(S)

12. DISTRIBUTION / AVAILABILITY STATEMENT

Approved for public release; distribution unlimited

13. SUPPLEMENTARY NOTES

14. ABSTRACT The overall objective of this project is to test the hypothesis that HOXC9 expression levels have a causal role in determining the differentiation states of neuroblastoma tumors, with higher levels of HOXC9 promoting differentiation. At the cellular level, HOXC9 promotes the differentiation and represses the self-renewal of neuroblastoma stem cells. At the molecular level, HOXC9 activates the H3K4 demethylase KDM5B and the H3K27 demethylase KDM6B for global control of its differentiation program. During the first budget year of this grant, significant progress has been made in the proposed studies, which is described in detail in the BODY section below. Briefly, we have submitted a manuscript reporting our new findings on the molecular mechanism by which HOXC9 induces neuronal differentiation of neuroblastoma cells. We show that HOXC9 directly regulate a large number of genes involved in neuronal differentiation, upregulating neuronal genes and downregulating cell cycle and DNA repair genes. We further present evidence for an essential role of E2F6 in HOXC9 repression of cell cycle genes and induction of G1 arrest. For Aim 1, we have generated MYCN mice (a mouse neuroblastoma model) with Hoxc9 deficiency or heterozygosity and initiated the study on their effects on neuroblastoma initiation and progression. For Aim 3, we have obtained evidence for critical roles of KDM5B and KDM6B in HOXC9 control of cell cycle and neuronal genes, respectively. These findings significantly advance our molecular understanding of neuroblastoma differentiation and suggest new targets for neuroblastoma therapy.

15. SUBJECT TERMS
Chromatin immunoprecipitation and sequencing, Epigenetics, Histone H3 methylation, Histone H3 demethylases (KDMs), HOXC9, Mouse model of neuroblastoma (MYCN mice), neuroblastoma differentiation

16. SECURITY CLASSIFICATION OF:			17. LIMITATION OF ABSTRACT	18. NUMBER OF PAGES	19a. NAME OF RESPONSIBLE PERSON
a. REPORT	b. ABSTRACT	c. THIS PAGE			USAMRMC
U	U	U	UU	57	19b. TELEPHONE NUMBER *(include area code)*

Table of Contents

Page

INTRODUCTION:

Neuroblastoma is a common pediatric cancer of the sympathetic nervous system [1]. It is a heterogeneous group of tumors, ranging from tumors composed predominantly of poorly differentiated neuroblasts to those consisting largely of differentiated neurons. Patients with poorly differentiated neuroblastoma have a significantly poorer prognosis than those with differentiated neuroblastoma. The molecular mechanisms underpinning neuroblastoma heterogeneity are largely unknown [2-5]. Our hypothesis is that HOXC9 expression levels have a causal role in determining the differentiation states of neuroblastoma tumors, with higher levels of HOXC9 promoting differentiation [6, 7]. At the cellular level, HOXC9 promotes the differentiation and represses the self-renewal of neuroblastoma stem cells. At the molecular level, HOXC9 activates the H3K4 demethylase KDM5B and the H3K27 demethylase KDM6B for global control of its differentiation program. The study supported by this award has three specific aims: **1) to investigate the role of HOXC9 in neuroblastoma development; 2) to investigate the role of HOXC9 in neuroblastoma stem cell differentiation;** and **3) to investigate the molecular mechanism for global control of HOXC9-induced differentiation.** Identification and characterization of neuroblastoma stem cells will advance our understanding of neuroblastoma heterogeneity and provide a key cellular target for earlier detection of neuroblastoma, for better prediction of clinical outcomes, and for cancer stem cell-based drug discovery. A molecular understanding of HOXC9-induced differentiation will open new avenues for the development of more effective differentiation-based neuroblastoma therapies.

BODY:

The timeline reflects potential 1-2 month delay to obtain ACURO approval.

Task 1. To investigate the role of HOXC9 in neuroblastoma development (months 3-26)

The goal of Task 1 is to test the hypothesis that HOXC9 expression levels have a causal role in determining the differentiation states of neuroblastoma tumors. We will examine the effects of Hoxc9 deficiency and heterozygosity on the differentiation states of neuroblastoma tumors developed in *MYCN* mice, an animal model of the human disease. As differentiation states affect tumor development, we will also examine the effects of Hoxc9 deficiency and heterozygosity on neuroblastoma initiation and progression in *MYCN* mice. A total of 492 mice will be used for breeding (n = 144, parental and F1 progeny) to generate the F2 progeny for the proposed hyperplasia and tumor development studies as outlined below:

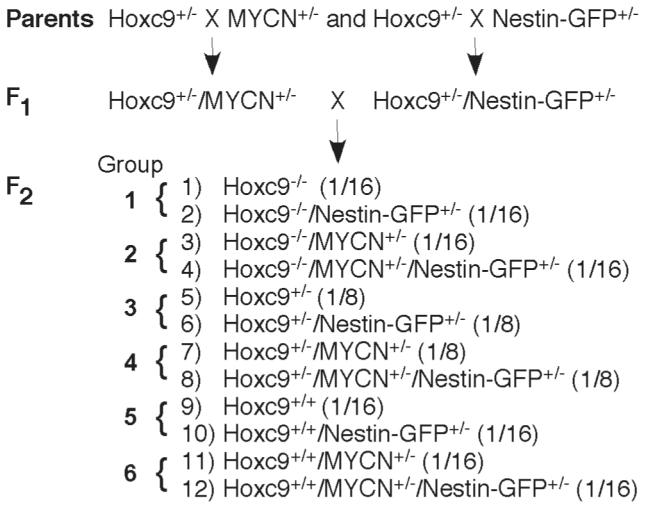

Fig. 1. Breeding scheme for the generation of Hoxc9-/-, Hoxc9+/- and Hoxc9+/+ mice with or without MYCN and/or Nestin-GFP transgenes. Numbers in Parentheses indicate the expected genotype frequencies.

a. Breeding (n = 144): Parental, 3 genotypes (Hoxc9+/-, MYCN+/-, nestin-GFP+/-), 28 mice/genotype, n = 84; F1, 2 genotypes (Hoxc9+/-/MYCN+/-, Hoxc9+/-/nestin-GFP+/-), 30 mice/genotype, n = 60.

b. Hyperplasia study (n = 108): 6 genotypes (Hoxc9+/+, Hoxc9+/-, Hoxc9-/- with or without MYCN and/or nestin-GFP), 18 mice/genotype.

c. Tumor development study (n = 240): 6 genotypes (same as above), 40 mice/genotype.

The Task 1 experiments outlined in the approved SOW for the first budget year include mouse breeding and hyperplasia formation studies.

1. Mouse breeding (months 3-12): $Hoxc9^{+/+}$, $Hoxc9^{+/-}$, and $Hoxc9^{-/-}$ mice with or without the *MYCN* and/or *nestin-GFP* transgene will be generated.

We have completed the breeding program and generated F2 progeny (i.e., Hoxc9$^{+/+}$, Hoxc9$^{+/-}$, and Hoxc9$^{-/-}$ mice with or without the *MYCN* and/or *nestin-GFP* transgene) for hyperplasia and tumor development studies (**Fig. 1**).

2. Hyperplasia formation studies (months 9-12): Superior cervical ganglia and celiac ganglia will be collected from mice (n = 6 mice per group x 6 groups =36) every week during the first 3 weeks after birth and sectioned for H&E and immunofluorescence staining for nestin, Phox2B and TH. The stained sections will be examined using regular and confocal fluorescent microscopes and positive cells will be quantified from randomly selected fields.

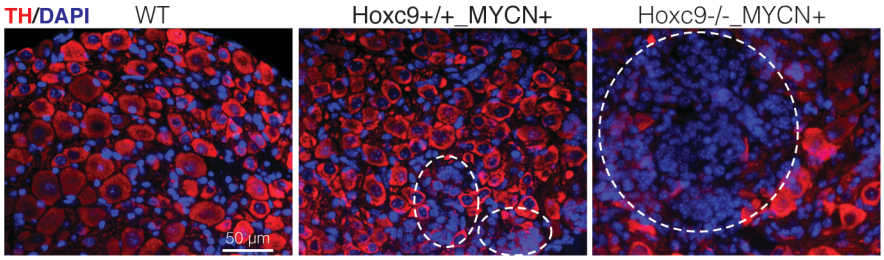

Fig. 2 Hoxc9 deficiency promotes neuroblastoma initiation in MYCN mice. Immunofluorescence staining for the sympathetic neuronal marker TH (red) in sections of sympathetic ganglia from 1-week-old WT, Hoxc9+/+ and Hoxc9-/- mice carrying the MYCN transgene. Nuclei were stained with DAPI. Hyperplastic lesions (clusters of undifferentiated, TH-negative cells) are marked by dashed circles.

We have finished the collection, section, and staining of superior cervical ganglia and celiac ganglia from Hoxc9$^{+/+}$, Hoxc9$^{+/-}$, and Hoxc9$^{-/-}$ mice with or without the *MYCN* and/or *nestin-GFP* transgene during the first 3 weeks after birth. As exemplified by data shown in Figure 2, immunofluorescence staining for TH (tyrosine hydroxylase, a sympathetic neuronal differentiation marker) revealed that hyperplastic lesions in sympathetic ganglia isolated from Hoxc9$^{-/-}$ mice expressing the *MYCN* transgene were markedly increased in size compared to those in sympathetic ganglia from Hoxc9$^{+/+}$/*MYCN* transgenic mice, demonstrating that Hoxc9 deficiency promotes hyperplasia formation. This finding provides the genetic evidence in support of our hypothesis that Hoxc9 suppresses neuroblastoma initiation.

No Task 2 experiments were planned during the first budget year.

Task 3. To investigate the molecular mechanism for global control of HOXC9-induced differentiation (months 3-32)

The goal of Task 3 is to test the hypothesis that HOXC9 transcriptionally activates the histone H3 demethylases KDM5B and KDM6B for global control of its differentiation program. It is well established that histone H3 methylation at specific lysine residues is a major mechanism for global control of development and differentiation programs by regulating the active and silent states of genes [8-10]. H3K4me3 maintains genes in an active state, whereas H3K27me3 keeps genes in a silent state. KDM5B catalyzes demethylation at H3K4, whereas KDM6B catalyzes demethylation at H3K27 [11, 12]. We proposed that KDM5B upregulation by HOXC9 leads to a decrease in H3K4me3 levels at cell cycle-promoting genes, whereas KDM6B upregulation by HOXC9 results in a decrease in H3K27me3 levels at the genes required for differentiation. This model was based on two lines of evidence. First, it has been shown that KDM5B functions as a negative regulator of cell cycle progression [13, 14]. Second, it has been shown that KDM6B is required for neuronal differentiation of embryonic stem cells [15, 16].

The Task 3 experiments outlined in the approved SOW for the first budget year include KDM5B and KDM6B overexpression studies, and some of KDM5B and KDM6B knockdown studies.

1. KDM5B and KDM6B overexpression studies (months 3-8): We will introduce KDM5B and KDM6B, individually or in combination, into BE(2)-C cells by lentiviral infection. These cells, along with their control GFP-expressing cells, will be examined for the expression of a panel of HOXC9 target genes involved in proliferation and differentiation (e.g. cyclins, Phox2B, and RET) by qRT-PCR and immunoblotting. We will also conduct functional analyses for the effects of KDM5B and KDM6B overexpression on cell proliferation and neuronal differentiation.

We have completed all the proposed studies as planned. For KDM5B overexpression studies, we have introduced KDM5B into the human neuroblastoma cell line BE(2)-C cells by lentiviral infection. Overexpression of KDM5B significantly repressed the expression of cyclins (**Fig. 3A**) and inhibited cell proliferation (**Fig. 3B-C**). These findings provide strong evidence in support of our hypothesis that HOXC9 activates KDM5B to repress cell growth-promoting genes and cell proliferation.

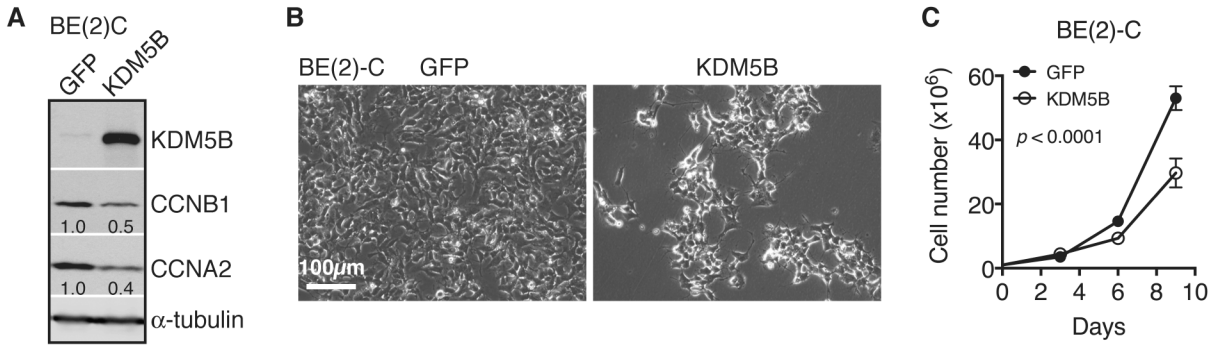

Fig. 3. KDM5B overexpression represses the expression of cyclins and inhibits neuroblastoma cell proliferation. **A,** Immunoblotting analysis of KDM5B, CCNB1 (cyclin B1), and CCNA2 (cyclin A2) in human neuroblastoma BE(2)-C cells overexpressing either GFP (control) or KDM5B. CCNB1 and CCNA2 levels were quantified against α-tubulin. **B,** Phase-contrast imaging of BE(2)-C cells overexpressing either GFP or KDM5B. **C,** Cell proliferation assay of BE(2)-C cells overexpressing either GFP or KDM5B. Overexpression of KDM5B significantly inhibits BE(2)-C cell proliferation. Data were analyzed by ANOVA (Analysis of Variance) with the p value indicated.

For KDM6B overexpression studies, we have introduced KDM6B into the human neuroblastoma cell line BE(2)-C cells by lentiviral infection. Overexpression of KDM6B had no apparent effect on cyclin B1 expression (**Fig. 4A**) and cell proliferation (data not shown), but significantly upregulated the expression of the neuronal genes *GFRA3, RET,* and *NEFM* (**Fig. 4B**). *GFRA3* encodes the glial cell line-derived neurotrophic factor (GDNF) family receptor alpha 3 (GFRα3), which forms a receptor complex with RET that preferentially binds the GDNF family ligand Artemin. This receptor signaling has a critical role in embryonic development of the sympathetic nervous system, promoting the differentiation and axonal outgrowth of sympathetic neurons [17]. NEFM (neurofilament, medium polypeptide 150kDa) is a common marker for differentiated neurons. These findings are consistent with our hypothesis that HOXC9 activates KDM6B to induce neuronal genes.

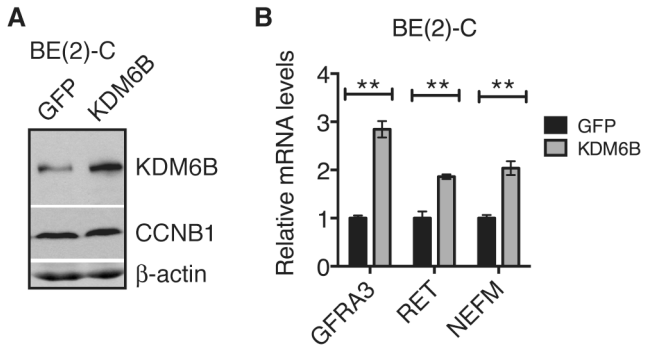

Fig. 4 KDM6B induces neuronal genes. A, Immunoblotting analysis of KDM6B and CCNB1 (cyclin B1) in human neuroblastoma BE(2)-C cells overexpressing either GFP (control) or KDM6B. β-actin levels are shown as loading control. **B,** qRT-PCR analysis of the mRNA expression of GFRA3, RET, and NEFM in BE(2)-C cells overexpressing either GFP or KDM6B. Data were analyzed by two-tailed Student's t-test. **p < 0.001.

2. <u>KDM5B and KDM6B knockdown studies (months 9-20)</u>:

a. To examine the effects of KDM5B and KDM6B knockdown on the induction of the HOXC9-induced differentiation program, we will infect BE(2)-C/Tet-Off/HOXC9 cells cultured in the presence of doxycycline (Doxy) with pLKO.1 lentiviral constructs expressing shRNA to human *KDM5B* or *KDM6B*. To examine the effects of KDM5B and KDM6B knockdown on the maintenance of the differentiation program, BE(2)-C/Tet-Off/HOXC9 cells will be cultured in the absence of Doxy for 6 days to induce HOXC9 and differentiation, followed by the lentiviral infection. pLKO.1-GFP shRNA will be used as negative control.

We have completed the study to examine the effect of KDM5B knockdown on the ability of HOXC9 to induce differentiation. We infected BE(2)-C/Tet-Off/HOXC9 cells cultured in the presence of doxycycline (Doxy) with

lentiviral constructs expressing shRNA to human *KDM5B*. Out of the five constructs, three were able to reduce KDM5B mRNA levels by 90% or more (**Fig. 5A**). The cells were then cultured in the absence of Doxy for 6 days to induce HOXC9. As expected, cells expressing GFP shRNA underwent G1 arrest following HOXC9 induction. In contrast, cells expressing KDM5B shRNA-62 were highly resistant to HOXC9-induced G1 arrest (**Fig. 5B**). Also, knockdown of KDM5B completely abolished the ability of HOXC9 to inhibit cell proliferation (**Fig. 5C**) and to repress cell cycle-promoting genes such as *CCNA2*, *CCNB1,* and *CCNE2* (**Fig. 5D**). Interestingly, KDM5B knockdown had no significant effect on the ability of HOXC9 to induce neuronal genes such as *RET* and *NEFM*, indicating that KDM5B specifically regulates the expression of cell cycle genes. We obtained similar results with cells expressing KDM5B shRNA-58 and KDM5B shRNA-61 (data not shown). Together, these findings indicate an essential role of KDM5B in mediating HOXC9-induced cell cycle arrest.

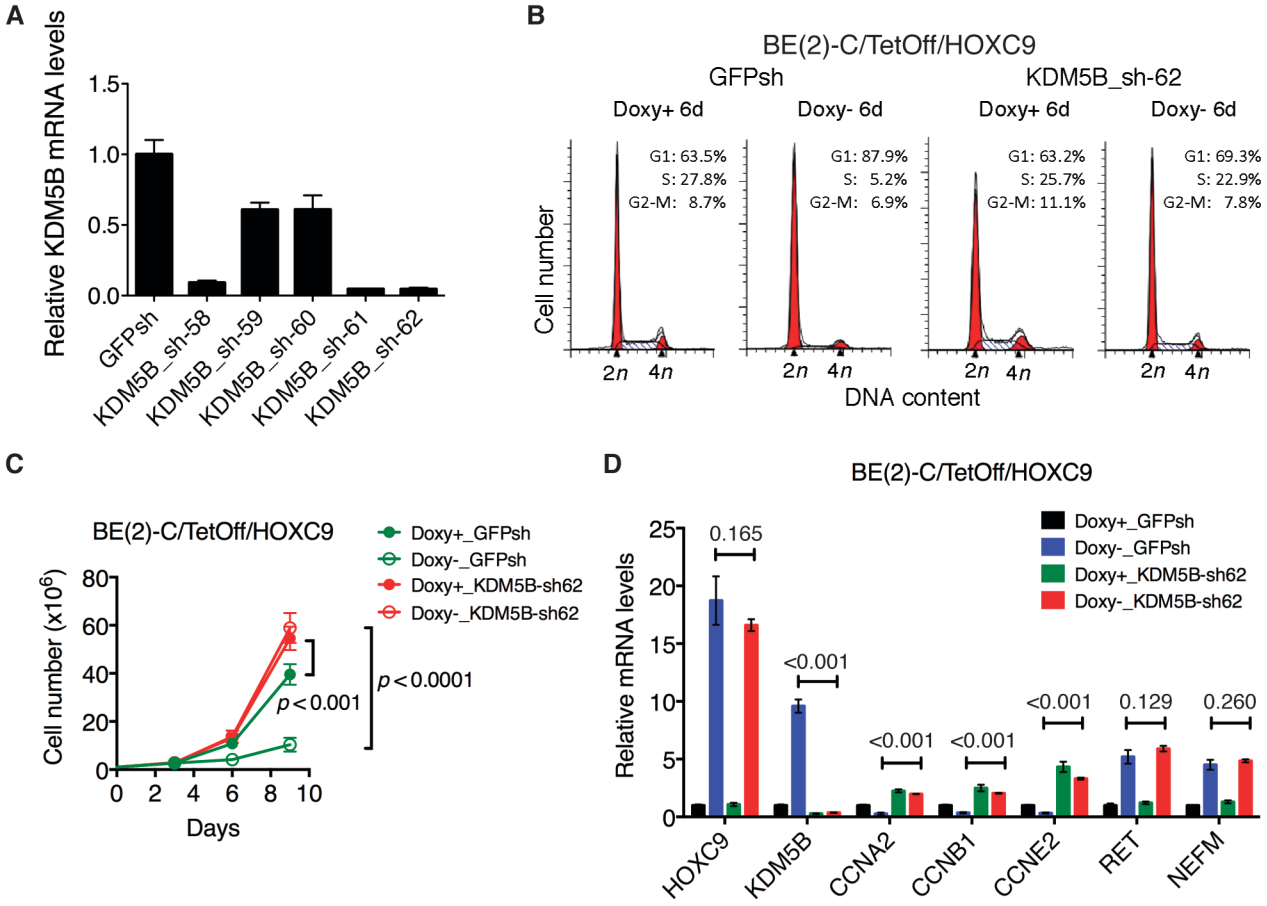

Fig. 5 KDM5B is essential for HOXC9 to inhibit cell proliferation and to repress the expression of cell cycle genes. **A,** qRT-PCR analysis of KDM5B mRNA levels in BE(2)-C/Tet-Off/HOXC9 cells infected with lentiviruses expressing shRNA against GFP (GFPsh) or KDM5B (KDM5Bsh). Error bars represent sem (n = 3). The KDM5B mRNA level in GFPsh cells was designated as 1.0. **B,** BE(2)-C/Tet-Off/HOXC9 cells expressing either GFPsh or KDM5B-sh62 were cultured in the presence or absence of doxycycline (Doxy) for 6 days, followed by cell cycle analysis. **C,** Cell proliferationassay of BE(2)-C/Tet-Off/HOXC9 cells expressing either GFPsh or KDM5B-sh62 that were cultured in the presence or absence of Doxy for various times, followed by trypan blue exclusion assay of viable cells. Data were analyzed by ANOVA with p values indicated. **D,** qRT-PCR analysis of the mRNA levels of the indicated genes in BE(2)-C/Tet-Off/HOXC9 cells expressing either GFPsh or KDM5B-sh62 that were cultured in the presence or absence of Doxy for 4 days. Data were analyzed by two-tailed Student's t-test, with p values indicated.

We have also begun KDM6B knockdown studies and are in the process of generating BE(2)-C/Tet-Off/HOXC9 cells expressing shRNA against KDM6B.

KEY RESEARCH ACCOMPLISHMENTS:

- We have completed the mouse-breeding program and generated the required F2 progeny for the proposed hyperplasia formation and tumor development studies.

- We have completed the hyperplasia formation study and obtained evidence showing that Hoxc9 deficiency enhanced hyperplasia formation in sympathetic ganglia of *MYCN* transgenic mice.

- We have completed the KDM5B overexpression study and obtained evidence showing that increased KDM5B expression inhibited cell proliferation and repressed the expression of cyclin genes.

- We have completed the KDM6B overexpression study and obtained evidence showing that increased KDM6B expression activated the expression of neuronal genes including *GRF3A, RET,* and *NEFM.*

- We have completed the KDM5B knockdown study and obtained evidence showing that KDM5B is essential for HOXC9 to induce G1 arrest and to repress the expression of cyclin genes, but is dispensable for HOXC9 to induce neuronal genes.

REPORTABLE OUTCOMES:

- Manuscripts, abstracts, presentations
    - Wang, X., Choi, J., Ding, J., Yang, L., Lee, E.J., Ngoka, Zha, Y., Jin, B., Ren, M., Huang, S., Cowell, J., Shi, H., Cui, H. **Ding, H.-F.** HOXC9 directly regulates distinct sets of genes to coordinate diverse cellular processes during differentiation. BMC Genomics. Revision.

- Patents and licenses applied for and/or issued
    - None

- Degrees obtained that are supported by this award
    - None

- Development of cell lines, tissue, or serum repositories
    - BE(2)-C/Tet-Off/HOXC9/KDM5B, BE(2)-C/Tet-Off/HOXC9/KDM6B, and BE(2)-C/Tet-Off/HOXC9/KDM5Bsh cell lines

- Informatics such as databases and animal models, etc.
    - $Hoxc9^{+/+}$, $Hoxc9^{+/-}$, and $Hoxc9^{-/-}$ mice with or without the *MYCN* and/or *nestin-GFP* transgene

- Funding applied for based on work supported by this award
    - None

- Employment or research opportunities applied for and/or received based on experience/training supported by this award
    - None

CONCLUSION:

Neuroblastoma is a common childhood malignant tumor of the sympathetic nervous system. Differentiation status in neuroblastoma strongly affects clinical outcomes and inducing differentiation is a treatment strategy in this disease [1-5]. We have recently shown that HOXC9 is a key regulator of neuroblastoma cell differentiation and a prognostic marker for survival in neuroblastoma patients [6]. Neuroblastoma differentiation is characterized at the molecular level by repression of cell cycle genes and activation of neuronal differentiation markers. Our research during the first budget year of this award has significantly advanced our understanding of the role and the mechanism of HOXC9 action in neuroblastoma. We found that Hoxc9 deficiency facilitated hyperplasia formation in sympathetic ganglia of *MYCN* transgenic mice, an animal model of human

neuroblastoma. We identified the H3K4 demethylase KDM5B as an essential downstream mediator of HOXC9 action in arresting cell cycle and repressing cell cycle genes. Importantly, overexpression of KDM5B alone was able to inhibit neuroblastoma cell proliferation. We also obtained evidence suggesting a key role of the H3K27 demethylase KDM6B in mediating the ability of HOXC9 to activate neuronal genes. These findings provide the first line of genetic evidence for a tumor-suppression function of Hoxc9 in neuroblastoma initiation and suggest that pharmacological activation of KDM5B is a potential therapeutic strategy for neuroblastoma.

REFERENCES:

1. Brodeur GM: **Neuroblastoma: biological insights into a clinical enigma.** *Nat Rev Cancer* 2003, **3:**203-216.
2. Beckwith JB, Martin RF: **Observations on the histopathology of neuroblastomas.** *J Pediatr Surg* 1968, **3:**106-110.
3. Hughes M, Marsden HB, Palmer MK: **Histologic patterns of neuroblastoma related to prognosis and clinical staging.** *Cancer* 1974, **34:**1706-1711.
4. Shimada H, Chatten J, Newton WA, Jr., Sachs N, Hamoudi AB, Chiba T, Marsden HB, Misugi K: **Histopathologic prognostic factors in neuroblastic tumors: definition of subtypes of ganglioneuroblastoma and an age-linked classification of neuroblastomas.** *J Natl Cancer Inst* 1984, **73:**405-416.
5. Ambros IM, Hata J, Joshi VV, Roald B, Dehner LP, Tuchler H, Potschger U, Shimada H: **Morphologic features of neuroblastoma (Schwannian stroma-poor tumors) in clinically favorable and unfavorable groups.** *Cancer* 2002, **94:**1574-1583.
6. Mao L, Ding J, Zha Y, Yang L, McCarthy BA, King W, Cui H, Ding HF: **HOXC9 Links Cell-Cycle Exit and Neuronal Differentiation and Is a Prognostic Marker in Neuroblastoma.** *Cancer Res* 2011, **71:**4314-4324.
7. Zha Y, Ding E, Yang L, Mao L, Wang X, McCarthy BA, Huang S, Ding HF: **Functional dissection of HOXD cluster genes in regulation of neuroblastoma cell proliferation and differentiation.** *PLoS One* 2012, **7:**e40728.
8. Schuettengruber B, Chourrout D, Vervoort M, Leblanc B, Cavalli G: **Genome regulation by polycomb and trithorax proteins.** *Cell* 2007, **128:**735-745.
9. Natoli G: **Maintaining cell identity through global control of genomic organization.** *Immunity* 2010, **33:**12-24.
10. Mills AA: **Throwing the cancer switch: reciprocal roles of polycomb and trithorax proteins.** *Nat Rev Cancer* 2010, **10:**669-682.
11. Swigut T, Wysocka J: **H3K27 demethylases, at long last.** *Cell* 2007, **131:**29-32.
12. Mosammaparast N, Shi Y: **Reversal of histone methylation: biochemical and molecular mechanisms of histone demethylases.** *Annu Rev Biochem* 2010, **79:**155-179.
13. Roesch A, Mueller AM, Stempfl T, Moehle C, Landthaler M, Vogt T: **RBP2-H1/JARID1B is a transcriptional regulator with a tumor suppressive potential in melanoma cells.** *Int J Cancer* 2008, **122:**1047-1057.
14. Roesch A, Becker B, Schneider-Brachert W, Hagen I, Landthaler M, Vogt T: **Re-expression of the retinoblastoma-binding protein 2-homolog 1 reveals tumor-suppressive functions in highly metastatic melanoma cells.** *J Invest Dermatol* 2006, **126:**1850-1859.
15. Burgold T, Spreafico F, De Santa F, Totaro MG, Prosperini E, Natoli G, Testa G: **The histone H3 lysine 27-specific demethylase Jmjd3 is required for neural commitment.** *PLoS One* 2008, **3:**e3034.
16. Dai JP, Lu JY, Zhang Y, Shen YF: **Jmjd3 activates Mash1 gene in RA-induced neuronal differentiation of P19 cells.** *J Cell Biochem* 2010, **110:**1457-1463.
17. Ernsberger U: **The role of GDNF family ligand signalling in the differentiation of sympathetic and dorsal root ganglion neurons.** *Cell Tissue Res* 2008, **333:**353-371.

APPENDICES:

- Wang, X., Choi, J., Ding, J., Yang, L., Lee, E.J., Ngoka, Zha, Y., Jin, B., Ren, M., Huang, S., Cowell, J., Shi, H., Cui, H. **Ding, H.-F.** HOXC9 directly regulates distinct sets of genes to coordinate diverse cellular processes during differentiation. BMC Genomics. Revision.

HOXC9 directly regulates distinct sets of genes to coordinate diverse cellular processes during neuronal differentiation

Xiangwei Wang[1,*], Jeong-Hyeon Choi[2,3,*], Jane Ding[2,4,*], Liqun Yang[6,*], Lambert C. Ngoka[2], Eun J. Lee[2,5], Yunhong Zha[7], Ling Mao[8], Bilian Jin[2,5], Mingqiang Ren[2,4], John Cowell[2,4], Shuang Huang[2,5], Huidong Shi[2,5], Hongjuan Cui[6,§] and Han-Fei Ding[2,4,5,§]

[1]Department of Urology, Second Affiliated Hospital, Third Military Medical University, Chongqing, China

[2]Cancer Center, [3]Department of Biostatistics and Epidemiology, [4]Department of Pathology, [5]Department of Biochemistry and Molecular Biology, Medical College of Georgia, Georgia Regents University, Augusta, GA 30912, USA

[6]State Key Laboratory of Silkworm Genome Biology, Institute of Sericulture and System Biology, Southwest University, Chongqing, China

[7]Department of Neurology, First Hospital of Yichang, Three Gorges University College of Medicine, Yichang, China

[8]Department of Neurology, Union Hospital, Tongji Medical College, Huazhong University of Science and Technology, Wuhan, China

*X.W., J.-H.C., J.D. and L.Y. contributed equally to this work.

[§]Correspondence: hding@gru.edu, Cancer Center, CN-2151, Georgia Regents University, 1120 15th Street, Augusta, Georgia 30912, USA; hcui@swu.edu.cn, State Key Laboratory of Silkworm Genome Biology, Institute of Sericulture and Systems Biology, Southwest University, 2 Tianshenqiao, Chongqing 400716, China.

Abstract

Background: Cellular differentiation is characterized by the acquisition of specialized structures and functions, cell cycle exit, and global attenuation of the DNA damage response. How these diverse cellular events are coordinated at the molecular level during differentiation is largely unknown. We addressed this question in a model system of neuroblastoma cell differentiation induced by HOXC9 [NP_008828].

Results: We have conducted a genome-wide analysis of the HOXC9-induced neuronal differentiation program. Microarray gene expression profiling reveals that HOXC9-induced differentiation is associated with transcriptional regulation of 2,370 genes, characterized by global upregulation of neuronal genes and downregulation of cell cycle and DNA repair genes. Remarkably, genome-wide mapping by ChIP-seq demonstrates that HOXC9 binds to 40% of these genes, including a large number of genes involved in neuronal differentiation, cell cycle progression and the DNA damage response. Moreover, we show that HOXC9 interacts with the transcriptional repressor E2F6 [NP_937987] and recruits it to the promoters of cell cycle genes for repressing their expression.

Conclusions: We delineate a molecular mechanism by which a single master regulator of development coordinates diverse cellular processes associated with differentiation by directly activating and repressing the transcription of distinct sets of genes.

Key words: Neuronal differentiation, cell cycle arrest, DNA damage response attenuation, E2F6, HOXC9, neuroblastoma.

Background

Cellular differentiation is an essential process of normal development by which a stem or progenitor cell becomes a post-mitotic, specialized cell with unique morphology and function. In addition, it has long been recognized that differentiated cells of both normal and tumor origin are defective in the DNA damage response and repair at the global level, displaying a marked increase in sensitivity to ionizing radiation and other DNA damaging agents [1-3]. Consistent with these observations, recent studies have shown that brain and breast cancer stem cells, a small subpopulation of tumor cells thought to be responsible for initiating and sustaining tumor growth [4-6], are more resistant to irradiation and chemotherapy than bulk tumor cells [7-10]. Particularly interesting is the observation that inhibition of DNA damage checkpoint kinases can reverse the radioresistance of glioma stem cells [7]. Thus, a molecular understanding of cellular differentiation may suggest new therapeutic strategies that target both cell proliferation and the DNA damage response.

Neuroblastoma is a common childhood malignant tumor of the sympathetic nervous system [11, 12]. Neuroblastoma cells can be induced to undergo neuronal differentiation by serum deprivation [13], nerve growth factor [14] or retinoic acid (RA) [15]. Fully differentiated neuroblastoma cells morphologically and functionally resemble mature peripheral neurons characterized by G1 arrest, extensive neurite outgrowth, and significant resting potential. It has long been observed that differentiated neuroblastoma cells are highly sensitive to UV and X-ray radiation with a significantly reduced rate of DNA damage repair [14, 16-19]. The molecular basis for the differentiation-induced radiosensitivity is not well understood.

RA has a key role in normal development of the nervous system [20, 21], and RA-induced neuronal differentiation of neuroblastoma cells is a well-established model for molecular investigation of neuronal differentiation [22]. We have shown recently that RA-induced differentiation of neuroblastoma cells requires the activation of several *HOX* genes [23, 24], a family of master regulators of morphogenesis and cell fate specification [25-27]. Among them, HOXC9 is a major mediator of RA action in neuroblastoma cells. HOXC9 expression is upregulated by RA, and silencing HOXC9 expression confers resistance to RA-induced differentiation. Importantly, ectopic HOXC9 expression alone is sufficient to induce growth arrest and morphologic differentiation in neuroblastoma cells, fully recapitulating the neuronal differentiation phenotype induced by RA [23].

The biological functions of RA are mediated by multiple isotypes of RA receptors (RARs) and retinoid X receptors (RXRs), which form RAR/RXR heterodimers that bind RA response elements in the regulatory regions of RA target genes and regulate their transcription [28]. The complexity of multiple RARs and RXRs involved in the action of RA presents a daunting challenge to dissect the molecular mechanism that coordinates the diverse cellular events associated with differentiation. Thus, the finding that HOXC9 alone is able to initiate a robust transcriptional program that drives neuronal differentiation provides a unique experimental system for this investigation. In this study, we conducted genome-wide profiling of the HOXC9-initiated transcriptional program. Our investigation reveals that HOXC9 directly regulates the expression of three major sets of genes that separately control neuronal differentiation, cell cycle progression, and the DNA damage response.

Results

Gene expression profiling of HOXC9-induced neuronal differentiation

To gain a molecular understanding of HOXC9-induced differentiation, we conducted microarray gene expression profiling of human neuroblastoma BE(2)-C/Tet-Off/myc-HOXC9 cells, which express myc-tagged human HOXC9 and undergo neuronal differentiation in the absence of doxycycline [23] (Figure 1A). The profiling analysis identified a total of 2,370 genes that were differentially expressed (≥ ±1.5 fold, P <0.01), with 879 genes being upregulated and 1,491 genes downregulated (Table S1 in Additional file 2). Gene annotation enrichment analysis revealed that HOXC9-induced differentiation is characterized by a genome-wide coordination in transcriptional regulation of genes that control neuronal differentiation, cell cycle progression, and the DNA damage response.

Global upregulation of neuronal genes. Gene Ontology (GO) analysis of the 879 HOXC9-upregulated genes by DAVID [29, 30] revealed that they were significantly enriched for genes that control nervous system development such as neuron generation and differentiation, axonogenesis, and synapse formation and organization (Figure 1B and Table S2 in Additional file 3, enrichment fold ≥ 2.0, false discovery rate (FDR) ≤1%). A total of 105 HOXC9-responsive genes were involved in nervous system development (Figure 1B), accounting for approximately 12% of the 879 genes upregulated by HOXC9. We obtained similar results with Gene Set Enrichment Analysis (GSEA), which showed significant enrichment of gene sets involved in synaptogenesis and neuron differentiation among the genes upregulated by HOXC9 (Figure 1C).

Particularly significant was the activation of *ASCL1*, *GFRA3, RET,* and *NTN3* (Figure 1D). ASCL1, a member of the basic helix-loop-helix (bHLH) family of transcription factors, is a master regulator in the generation and differentiation of sympathetic neurons [31, 32]. *GFRA3* encodes the glial cell line-derived neurotrophic factor (GDNF) family receptor alpha 3 (GFRα3), which forms a receptor complex with RET that preferentially binds the GDNF family ligand Artemin. This receptor signaling has a critical role in embryonic development of the sympathetic nervous system, promoting the survival, differentiation, axonal outgrowth, and target innervation of sympathetic neurons [33]. NTN3 (netrin 3) belongs to a family of extracellular proteins that promote axon growth and migration during the development of the nervous system [34]. Ingenuity Pathways Analysis (IPA) further revealed a network of HOXC9-upregulated genes relevant to the development and function of sympathetic neurons (Figure S1, Additional file 1). Together, these analyses demonstrate that HOXC9 activates a large number of neuronal genes, providing the molecular mechanism for its ability to induce neuronal differentiation of neuroblastoma cells.

Global downregulation of cell cycle and DNA repair genes. GO analysis of the 1,491 HOXC9-downregulated genes revealed that they were remarkably enriched for genes that control cell cycle progression and the DNA damage response (Figure 2A and Table S3 in Additional file 4, enrichment fold $\geq$ 2.0; FDR $\leq$1%). The analysis identified 206 genes involved in cell cycle regulation and 98 genes in the DNA damage response (Figure 2A). Similarly, GSEA showed that among the genes downregulated by HOXC9, those controlling mitotic cell cycle, DNA replication and DNA repair were significantly enriched (Figure 2B). IPA further revealed that the downregulated genes

include most of cyclin (CCN) and cyclin-dependent kinase (CDK) genes, and genes that control DNA replication, mitosis, double-strand break (DSB) repair, base excision repair (BER), nucleotide excision repair (NER), mismatch repair (MMR), and Fanconi anemia (FA)-mediated repair (Figures S2A-S2E in Additional file 1 and Table S3 in Additional file 4). These findings suggest that global downregulation of cell cycle and DNA repair genes is the primary cause of the cell cycle arrest and attenuation of the DNA damage response associated with HOXC9-induced neuronal differentiation.

Genome-wide mapping of HOXC9-binding sites

We next asked how HOXC9 coordinates the expression of distinct sets of genes: the upregulation of genes critical for nervous system development and the downregulation of genes essential for cell cycle progression and the DNA damage response. Mechanistically, HOXC9 could function through a few master transcription factors, which in turn regulate their own subsets of target genes that work together to drive differentiation. Alternatively, HOXC9 could directly regulate distinct sets of genes to coordinate the cellular events associated with differentiation. To test these models, we conducted two independent anti-HOXC9 chromatin immunoprecipitation assays followed by massively parallel sequencing of the enriched DNA fragments (ChIP-seq) for genome-wide mapping of HOXC9-binding sites. We identified a total of 29,221 HOXC9-binding peaks with FDR less than 1% (Figure 3A and Table S4 in Additional file 5). Scatter plot analysis (Figure 3B, R = 0.93, correlation coefficient) and ChIP-seq tag profiles (Figure 3C) demonstrated that the mapping data were highly reproducible between the two independent HOXC9 ChIP-seq samples. Genome-wide distribution

analysis of the binding peaks revealed that HOXC9 was predominantly associated with introns (41.2%) and intergenic regions (43.4%) (Figure 3D). A total of 4,992 genes were identified that contained at least one HOXC9-binding peak within 5-kb upstream or downstream of their genomic loci (Figure 3A and Table S5 in Additional file 6). The HOXC9-binding peaks were highly enriched in promoter regions, defined as those within 5 kb upstream of TSS of genes (Figure 3E). Analysis of the sequences covered by HOXC9-binding peaks with the motif-finding program MEME revealed that the most enriched binding motif (E value = 1.6e-35) is highly homologous to the *Drosophila* Abd-B motif (MA0165.1, Figure 3F). HOXC9 is a mammalian ortholog of the *Drosophila* Hox protein Abd-B. Thus, myc-tagged HOXC9 binds to cognate sequences in human neuroblastoma cells.

Genome-wide identification of HOXC9 target genes

We combined the anti-HOXC9 ChIP-seq data with the HOXC9 microarray data to generate a list of genes that were bound by HOXC9 and whose expression levels were significantly changed as a result of HOXC9 induction (≥ ±1.5 fold, P <0.01). The analysis revealed that 954 genes or 40.3% of the 2,370 HOXC9-responsive genes are direct targets of HOXC9, with 445 and 509 genes being upregulated and downregulated, respectively (Table S6 in Additional file 7). GO analysis of HOXC9 direct target genes revealed a transcriptional program characterized by coordinated regulation of genes critical for neuron differentiation, cell cycle progression, and the DNA damage response.

HOXC9 directly induces a large number of neuronal genes. The only sets of genes that were significantly enriched among the upregulated HOXC9 target genes are those exclusively involved in nervous system development, particularly the generation and differentiation of neurons and axonogenesis (Figure 4A and Table S7 in Additional file 8, enrichment fold ≥ 2.0, FDR ≤ 5%). The 57 HOXC9 direct target genes account for 54.3% (57/105) of the HOXC9-responsive genes involved in nervous system development (Figure 1B). Among them are *ASCL1, GFRA3, RET,* and *NTN3*. Figure 4B shows the ChIP-tag profiles of HOXC9 binding to the promoter regions of *GFRA3, RET,* and *NTN3*. As discussed above, these genes have a critical role in sympathetic neurogenesis and axonogenesis.

HOXC9 directly represses a large number of genes essential for cell cycle progression and the DNA damage response. GO analysis of the downregulated HOXC9 target genes revealed that they were significantly enriched for genes that control cell cycle progression and the DNA damage response (Figure 5A and Table S8 in Additional file 9), enrichment fold ≥ 2.0, FDR ≤ 1%). The analysis identified 52 cell cycle genes that were directly repressed by HOXC9 (Figure 5A), accounting for 25.2% (52/206) of the HOXC9-responsive genes involved in cell cycle regulation (Figure 2A). It was particularly striking that the vast majority of the HOXC9-repressed cell cycle genes are involved in the control of the M phase (n = 25) and DNA replication (n = 21) (Figure 5A). Figures 5B and 5C show the association of HOXC9 with the promoter regions of representative cell cycle genes, including *CDC45L* and *MCM3* (DNA replication), and *CCNB1* and *CDCA8* (M phase). CDC45L and MCM3 are components of the replicative complex that catalyzes DNA replication during the S phase [35], while CDCA8, also

known as BOREALIN, is a component of the chromosomal passenger complex essential for mitosis and cell division [36].

We also identified 32 genes associated with the DNA damage response that were directly repressed by HOXC9 (Figure 5A), accounting for 32.7% (32/98) of the HOXC9-responsive genes involved in the DNA damage response. Figure 5D shows the binding of HOXC9 to the promoter of *FANCM* and to both the promoter and 3' region of *FEN1*. FANCM is a component of the FANCM–FAAP24–MHF protein complex that binds to DNA with interstrand cross-links and is responsible for recruiting the FA core complex to the damaged site [37]. FEN1 (flap endonuclease 1) is essential for DNA replication and repair by removing RNA and DNA 5' flaps [38].

Collectively, these findings suggest that HOXC9 directly regulates the expression of distinct sets of genes to coordinate the molecular and cellular processes characteristic of neuronal differentiation.

HOXC9 targets E2F6 to the promoters of cell cycle genes

We next sought to determine the molecular basis for HOXC9 regulation of gene expression by identifying HOXC9-interacting proteins. We used a myc-tag antibody to isolate myc-HOXC9 and its associated proteins from nuclear extracts of BE(2)-C/Tet-Off/myc-HOXC9 cells cultured in the absence of doxycycline for 6 days (Figure S3A in Additional file 1). Mass spectrometric analysis of two independent samples identified E2F6 as a HOXC9-interacting protein (Figure S3B in Additional file 1), a well characterized transcriptional repressor that plays a major role in repressing E2F-responsive genes essential for cell proliferation [39]. It is known that E2F family proteins

(E2F1-6) share the same core consensus G/CTTTG/C binding site [40]. Interestingly, GSEA revealed significant enrichment of the E2F-binding motif among the genes downregulated by HOXC9 (Figure S3C in Additional file 1). Taken together, these observations suggest that E2F6 may have an important role in HOXC9-mediated repression of cell cycle genes.

To corroborate the finding of mass spectrometry, we performed co-immunoprecipitation (Co-IP) experiments using nuclear extracts from BE(2)-C/Tet-Off/myc-HOXC9 cells cultured in the absence of doxycycline for 6 days. The myc-tag antibody, but not control IgG, precipitated myc-HOXC9 and E2F6 (Figure 6A, left panel). Reciprocally, an E2F6 antibody precipitated E2F6 and myc-HOXC9 (Figure 6A, right panel). We next performed size-exclusion chromatography using the same nuclear extracts. Immunoblot analysis revealed the presence of HOXC9 (~31 kDa) in two complexes: the larger complex (peak at fraction 20) had an estimated molecular mass of ~1,800 kDa and the other (peak at fraction 34) of ~250 kDa (Figure 6B). A significant amount of endogenous E2F6 (~36 kDa) co-eluted with the 1,800-kDa HOXC9 complex, whereas MEIS2 (~37-49 kDa), which interacts with HOX proteins and functions as a HOX cofactor [26], exclusively co-eluted with the 250 kDa-HOXC9 complex (Figure 6B). Co-IP experiments using pooled fractions confirmed the association of HOXC9 with E2F6 within the larger complex (Figure 6C).

To determine whether the HOXC9-E2F6 interaction plays a role in recruiting E2F6 to HOXC9 target genes in vivo, we performed anti-E2F6 ChIP using BE(2)-C/Tet-Off/myc-HOXC9 cells before and after HOXC9 induction. ChIP-qPCR assay revealed that E2F6 was recruited to specific promoter regions of the cell cycle genes *CCNB1* and

CDCA8 only after HOXC9 induction (Figure 6D). By contrast, no significant binding of E2F6 to the *NEFM* promoter was observed before and after HOXC9 induction (Figure S4A in Additional file 1). As reported previously, *NEFM* is a neuronal gene directly activated by HOXC9 during differentiation [23] (See also Figure S4B in Additional file 1). Together, these data indicate that HOXC9 forms a repressive complex with E2F6 and recruits it to cell cycle but not neuronal genes during differentiation.

E2F6 is essential for HOXC9-induced cell cycle arrest and transcriptional repression of cell cycle genes

To determine the functional significance of the HOXC9-E2F6 interaction, we examined the effect of E2F6 knockdown on HOXC9-induced growth arrest. We depleted E2F6 using short hairpin RNA (shRNA) sequences targeting different coding regions of the human *E2F6* gene (Figure 7A). Cells with E2F6 knockdown were highly resistant to HOXC9-induced G1 arrest, showing continued cell proliferation (Figure 7B) and cell cycle progression (Figure 7C) following HOXC9 induction. This was accompanied by a marked decrease in the population of cells in the G1 phase and a significant increase in the population of cells in the S phase (Figure 7D). In addition, E2F6 knockdown largely abrogated the ability of HOXC9 to repress cyclin A2 and B1 expression, but had no significant effect on HOXC9 induction of NEFM (Figures 7E and 7F), a finding consistent with the observation of no significant E2F6 binding to the *NEFM* promoter during HOXC9-induced differentiation (Figure S4A in Additional file 1). Together, these findings identify an essential and specific role for E2F6 in HOXC9 induction of growth arrest and repression of cell cycle genes.

DISCUSSION

In this report, we present evidence for a master regulator of development with the capacity to coordinate diverse cellular events characteristic of neuronal differentiation by simultaneously and directly regulating distinct sets of genes (Figure 8). Through gene expression profiling, we show that HOXC9-induced neuronal differentiation is characterized at the molecular level by transcriptional regulation of 2,370 genes, with global upregulation of genes that promote nervous system development and downregulation of genes that are essential for cell cycle progression and the DNA damage response. Moreover, through a combination of genome-wide mapping of HOXC9 binding sites and gene expression profiling, we show that HOXC9 directly regulates the expression of 954 genes, ~40% of the 2,370 HOXC9-responsive genes, including a large number of genes required for neuronal differentiation, cell cycle progression and the DNA damage response. Finally, we identify an essential role for E2F6 in HOXC9 repression of cell cycle genes and induction of G1 arrest.

Cellular differentiation is tightly linked to cell cycle exit, with the differentiated cell containing the G1 content of DNA. The molecular mechanism that couples cell cycle exit and differentiation is not well understood, although it is generally recognized that cell cycle regulators influence differentiation, and cell fate determinants influence the cell cycle [41-44]. A primary example is the CDK inhibitor $p27^{Kip1}$ as a key regulator that links cell cycle exit and differentiation during development. $p27^{Kip1}$ induces G1 arrest by associating with CDK/cyclin complexes and inhibits their kinase activity [45]. Overexpression of $p27^{Xic1}$, a *Xenopus* homolog of $p27^{Kip1}$, in *Xenopus* retina glial

progenitor cells promotes both cell cycle exit and differentiation [46]. Knockout and overexpression studies also demonstrate an important role of $p27^{Kip1}$ in neuronal differentiation in the mouse cerebral cortex by stabilizing Neurogenin 2 [47], a proneural bHLH transcription factor with a central role in cortical neurogenesis [48]. On the other hand, cell fate determinants can also modulate the expression of $p27^{Kip1}$ for coordinated regulation of cell cycle exit and differentiation. For instance, *Drosophila* proneural bHLH proteins cooperate with epidermal growth factor signaling to directly activate the transcription of *Dapaco*, a homolog of $p21^{Cip}$/$p27^{Kip1}$, during the differentiation of photoreceptor cells [49].

Our findings suggest an alternative mechanism for coupling cell cycle exit and differentiation. HOXC9 does not regulate the expression of CDK inhibitors, including $p27^{Kip1}$ and $p21^{Cip}$, and overexpression of either $p27^{Kip1}$ or $p21^{Cip}$ fails to stop the proliferation of BE(2)-C cells [23]. Rather, HOXC9 induces G1 arrest by directly repressing a large number of genes essential for cell cycle progression through the S to M phases, including cyclin B1, CDCA3, CDCA8, BUB1B, MCM3 and MCM8. This transcriptional repression function of HOXC9 requires E2F6, a member of the E2F family of transcription factors that have a critical role in regulation of cell proliferation. We found that HOXC9 interacts with E2F6 and recruits it specifically to the promoters of cell cycle genes. E2F6 lacks a transactivation domain and functions as a transcriptional repressor for E2F-responsive genes that drive cell proliferation [50-54]. Mechanistically, E2F6 interacts with chromatin modifiers with transcriptional repressor activity to establish a repressive chromatin structure. These chromatin modifiers include the DNA methyltransferase Dnmt3b [55] and polycomb-group (PcG) proteins [56-59]. In our

study, we identified HOXC9 and E2F6 within a complex of approximately 1,800 kDa. Whether this complex contains chromatin modifiers is currently under investigation.

Terminal cell differentiation is also tightly associated with a global reduction in DNA damage repair activities [1-3]. However, the underlying molecular mechanism is not well understood. It has been reported that E1 ubiquitin-activating enzyme can complement nucleotide-excision repair deficiency in extracts from differentiated macrophages, suggesting a role of ubiquitination in the control of DNA damage response during differentiation [60]. Our study reveals that in HOXC9-induced neuronal differentiation, attenuation of the DNA damage response results from global transcriptional repression of DNA repair genes. This finding provides a molecular mechanism for the long observed differentiation-induced radiosensitivity in neuroblastoma cells [14, 16-19]. For HOXC9-induced differentiation, a total of 98 genes with functions in the DNA damage response were significantly downregulated. These genes are involved in all types of DNA damage checkpoints and repair pathways. Importantly, we show that 32 of the 98 genes are direct targets of HOXC9. Thus, to a large extent, HOXC9 coordinates neuronal differentiation and attenuation of DNA repair activities by simultaneously activating neuronal genes and repressing DNA repair genes. Since the DNA damage response and DNA replication machineries share many components, we speculate that the downregulation of DNA repair genes during differentiation is a consequence of repression of the cell cycle genes, particularly those involved in DNA replication.

The stem cell model of cancer attributes cancer growth to a subpopulation of cancer stem cells. It has been shown recently in several types of cancers that these

cancer stem cells are intrinsically resistant to ionizing radiation and chemotherapy, as a result of enhanced checkpoint activation and more effective DNA damage repair [7-10]. Since differentiation is associated with global downregulation of DNA repair activities, a combination of differentiation-inducing agents and irradiation or chemotherapy may prove to be a more effective therapeutic strategy for targeting cancer stem cells.

Conclusions

We delineate a molecular mechanism by which a single master regulator of development coordinates diverse cellular processes associated with differentiation by directly activating and repressing the transcription of distinct sets of genes.

Materials and Methods

Cell culture and growth assays

The human neuroblastoma cell line BE(2)-C (CRL-2268, ATCC) with Tet-Off inducible expression of myc-tagged human HOXC9 has been described previously [23]. For E2F6 knockdown, BE(2)-C/Tet-Off/myc-HOXC9 cells were infected with lentiviruses expressing shRNA against E2F6 (TRCN013819, E2F6sh-2, TTTCGAGTTAAATAAACCAGC; TRCN013821, E2F6sh-4, ATTGGTGATGTCATACACTCT; TRCN018201, E2F6sh-6, ATCCAAAGCATCTTCCATTGC; Thermo Fisher Scientific). Cells were cultured in a 1:1 mixture of DMEM and Ham's nutrient mixture F12 supplemented with 10% fetal bovine serum (Invitrogen-Gibco) in the presence or absence of doxycycline. Cells were examined and phase contrast images captured using an Axio Observer microscope and

AxioVision software (Carl Zeiss MicroImaging), and viable cell numbers were determined by trypan blue exclusion assay. For cell cycle analysis, cells were fixed in 70% ethanol, incubated with ribonuclease A (Sigma-Aldrich), and stained with 20 µg/ml propidium iodide (Invitrogen-Gibco). Samples were analyzed using a FACSCalibur system and ModFitLT V3.2.1 software (BD Bioscience).

Microarray gene expression profiling

Total RNA was isolated using Trizol (Invitrogen) from three independent samples of BE(2)-C/Tet-Off/myc-HOXC9 cells cultured in the presence or absence of doxycycline for 6 days. RNA was measured and quality assessed by a NanoDrop spectrophotometer and an Agilent 2100 Bioanalyzer (Agilent Technologies). Affymetrix microarray analysis was performed using the Human Gene 1.0 ST microarray chip. Data were normalized, significance determined by ANOVA, and fold change calculated with the Partek Genomics Suite (Partek Inc.). Gene annotation enrichment analysis was performed with DAVID v6.7 [30], GSEA [61], and IPA (Ingenuity® Systems www.ingenuity.com) for all significantly changed genes (≥ ±1.5 fold, $P < 0.01$).

ChIP-seq and ChIP-qPCR

Two independent preparations of BE(2)-C/Tet-Off/myc-HOXC9 cells cultured in the presence or absence of doxycycline for 6 days were used for ChIP. Cross-linked chromatin DNA was sheared through sonication and immunoprecipitated using mouse anti-myc tag (clone 4A6, Millipore) or mouse anti-E2F6 (sc-53273, Santa Cruz Biotechnologies) according to the published procedure [62]. For ChIP-seq, libraries

were generated from ChIP genomic DNA samples according to the Illumina ChIP-seq library construction procedure, and sequenced using Illumina Genome Analyzer IIx with a read length of 36 or 76 bp. For ChIP-qPCR, ChIP genomic DNA samples were assayed in triplicate by PCR using an iQ5 real-time PCR system (Bio-Rad) and the following primer sets that cover the promoter regions of *CCNB1* (CCNB1_2 and CCNB1_6), *CDCA8* (CDCA8_5P200 and CDCA8_5P1K), and *NEFM* (NEFM_5P1 and NEFM_5P2): CCNB1_2: CCAGAGAGTTGTTGCAACGAT, CTGGAGAGCAGTGAAGCCAGT; CCNB1_6: GGAAGGATTGATCAAACCCAG, AGTCACGGATCCGAAAGAAGG; CDCA8_5P200: GGTATTGCAGAGCCGCCA, CCTCCCCACCAACCCACC; CDCA8_5P1K: TGGTGCCCATCAGGAGCC, GGCTATGGGAGTGATAATC; NEFM_5P1: GCAGAAAGTAATAAGCAACAA, CCTGCCTTCTGTAAAGTATTG; NEFM_5P2: CCTTTCCTGATTACTTACTGA, AGGGACTCCAGACCGAAATAG.

ChIP-seq data analysis

Raw Illumina sequencing reads in the FASTQ format were cleaned using in-house scripts by trimming sequencing adaptors and low quality bases in both ends (Q<67 in Illumina 1.5). Cleaned sequences were then mapped to the human genome (hg19) using Novoalign v2.07. The reads that mapped uniquely to a single genomic locus were used for peak finding with Model-based Analysis of ChIP-Seq (MACS v1.4) [63], and only those peaks with FDR <1% were compared with RefSeq genes in the UCSC genome browser and classified into functional categories such as promoters (within 5 kb upstream of the transcription start site, TSS), 5’ untranslated regions (UTRs), exons,

introns, 3' UTRs, downstream (within 5-kb downstream of the gene), and intergenic regions (outside -5 ~ +5 kb of genes). To measure the correlation of two HOXC9 replicates, we used 200 bp non-overlapping windows where a tag density is defined as the number of reads in a window. We calculated Pearson correlation coefficient with R > 0.9 being highly correlated. For motif analysis, we extracted 100 bp flanking sequences from predicted peak summits and ran MEME for identifying statistically overrepresented motifs. We performed MAST to search motifs in the peaks using the model built by MEME.

Identification of HOXC9 target genes

Genes with HOXC9-binding peaks that are non-intergenic (i.e., within -5 ~ +5 kb of genes) were defined as HOXC9 target genes. To correlate HOXC9 binding to gene expression, we combined the HOXC9 ChIP-seq data with the HOXC9 microarray data using in-house scripts to generate a list of the genes whose regulatory elements are bound by HOXC9 and whose expression levels are significantly changed (≥ ±1.5 fold, $P < 0.01$) as the result of HOXC9 induction. The significantly up- and down-regulated HOXC9 target genes were then subjected to gene annotation enrichment analysis with DAVID v6.7, GSEA, and IPA.

Immunoprecipitation and mass spectrometric analyses

BE(2)-C/Tet-Off/myc-HOXC9 cells were cultured in the absence of doxycycline for 6 days and nuclear extracts were prepared following the Dignam protocol [64] except that buffer C contained 300 mM NaCl. Extracts from 1 x 10^7 cells were incubated with

Protein A/G beads (Invitrogen) coated with 4 µg mouse anti-Myc tag (clone 4A6, Millipore) or mouse IgG for overnight at 4^{o}C. The beads were washed 3 times with buffer C containing 150 mM NaCl, dried in a SpeedVac, re-suspended in a buffer containing 8M urea, 5 mM DTT and 100 mM ammonium bicarbonate, and alkylated with 15 mM iodoacetamide for 1 hour. After alkylation, unreacted iodoacetamide was removed by 15 mM DTT and the urea concentration was diluted to ~1M with a buffer containing 50 mM ammonium bicarbonate and 2 mM $CaCl_2$. Immunoprecipitated proteins were digested with 14 ng/µl sequencing grade trypsin (Promega) for 24 hours at 37°C. The digests were desalted with a Micro Trap desalting cartridge (Michrom BioResources), and tryptic peptides eluted with LC-MS Solvent B (90/10/0.05%: Acetonitrile/water/heptafluorobutyric acid) and dried in a SpeedVac. The digests were analyzed by Nano-HPLC using a Nano Trap column (CL5/61241/00, Michrom BioResources) and an Agilent 1200 Series Nano pump (Agilent Technologies) equipped with a refrigerated autosampler. An Agilent 1200 Series Capillary LC loading pump was used to introduce the sample onto a Captrap cartridge for sample concentration and de-salting.

Data-dependent MS and MS/MS spectra were acquired on an LTQ Orbitrap Discovery (Thermo Fisher Scientific) using 2 micro-scans, with a maximum injection time of 200 ms with 2 Da peak isolation width. Six scan events were recorded for each data acquisition cycle. The first scan event, acquired by the FTMS, was used for full scan MS acquisition from 300-2000 *m/z*. Data were recorded in the Centriod mode only. The remaining five scan events were used for collisionally activated dissociation (CAD):

the five most abundant ions in each peptide MS were selected and fragmented to produce product-ion mass spectra.

Database searching and protein identification

All MS/MS data were analyzed using BioWorks Rev.3.3.1 SP1 (Thermo Fisher Scientific) and X!Tandem (thegpm.org). SEQUEST was set up to search NCBInr_Homosapiens_05262011.fasta (221863 entries) and the human.protein_RefSeq_01192012 database (33376), and X!Tandem was set up to search subsets of the databases. SEQUEST and X!Tandem were searched with a fragment ion mass tolerance of 0.80 Da and a parent ion tolerance of 10.0 PPM. Scaffold (Proteome Software) was used to validate MS/MS-based peptide and protein identifications. Peptide identifications were accepted if they could be established at greater than 95.0% probability as specified by the Peptide Prophet algorithm [65]. Protein identifications were accepted if they could be established at greater than 90.0% probability and contained at least 1 identified peptide. Protein probabilities were assigned by the Protein Prophet algorithm [66]. Proteins that contained similar peptides and could not be differentiated based on MS/MS analysis alone were grouped to satisfy the principles of parsimony. Single-peptide protein identification was accepted only if the protein was independently identified by both SEQUEST and X!Tandem.

Size-exclusion chromatography

Size-exclusion chromatography was performed with a Superose-6 10/300 GL column (24 ml bed volume) and an AKTA purifier (GE Healthcare). Nuclear extracts (0.5 ml)

were loaded onto the column equilibrated with PBS, and 0.5 ml fractions were collected and analyzed.

Co-immunoprecipitation

Nuclear extracts or pooled Sepharose-6 fractions were incubated with protein A/G beads coated with mouse anti-Myc tag (clone 4A6), mouse anti-E2F6, or control mouse IgG for 2 hours at 4^{o}C. After washing 3 times with PBS, the beads were suspended in standard SDS sample buffer and analyzed by immunoblotting.

Immunoblotting

Unless indicated, all antibodies were from Santa Cruz Biotechnologies. Samples were suspended in SDS sample buffer and boiled. Proteins were separated on SDS-polyacrylamide gels, transferred to nitrocellulose membranes, and probed with the following primary antibodies: rabbit anti-cyclin A2 (sc-751, 1:200), rabbit anti-cyclin B1 (sc-752, 1:200), mouse anti-myc-tag (9E10, hybridoma supernatant, 1:10), rabbit anti-E2F6 (sc-22823, 1:200), mouse anti-MEIS2 (63-T, sc-81986, 1:400), mouse anti-NEFM (NF-09, sc-51683, 1:200), and rabbit anti-β-actin (600-401-886, Rockland Immunochemicals, 1:2000). Horseradish peroxidase-conjugated goat anti-mouse and goat anti-rabbit IgG were used as secondary antibodies. Proteins were visualized using a SuperSignal West Pico chemiluminescence kit (Pierce, Thermo Fisher Scientific) and quantified with ImageJ (National Institutes of Health). For visualization and quantification with the Odyssey system, goat anti-mouse IRDye 800, anti-rabbit IRDye

800, anti-mouse IRDye 680, and anti-rabbit IRDye 680 were used as secondary antibodies (LI-COR Biosciences).

Statistics

All quantitative data were analyzed and presented with GraphPad Prism 5.0f for Mac using unpaired, two-tailed Student's *t*-test.

Additional material

The following additional data are available with the online version of this paper:

Additional file 1: Figures S1-S4.

Additional file 2: Table S1_HOXC9-responsivel genes.

Additional file 3: Table S2_GO analysis of upregulated HOXC9-responsive genes.

Additional file 4: Table S3_GO analysis of downregulated HOXC9-responsive genes.

Additional file 5: Table S4_HOXC9-binding peaks.

Additional file 6: Table S5_HOXC9-binding genes.

Additional file 7: Table S6_HOXC9-target genes.

Additional file 8: Table S7_GO analysis of upregulated HOXC9 direct target genes.

Additional file 9: Table S8_GO analysis of downregulated HOXC9 direct target genes.

Abbreviations

BER: base excision repair; CCN: cyclin; CDK: cyclin-dependent kinase; ChIP-seq: Chromatin immunoprecipitation and sequencing; Co-IP: co-immunoprecipitation; DAVID: Database for annotation, visualization and integrated discovery; DMEM:

Dulbecco's Modified Eagle Medium**;** DSB; double-strand break; FA: Fanconi anemia; FDR: false discovery rate; GSEA: Gene Set Enrichment Analysis; IPA: Ingenuity Pathways Analysis; LC-MS: Liquid Chromatography - Mass Spectrometry; MMR: mismatch repair; NEFM: neurofilament medium; NER: nucleotide excision repair; PBS: Phosphate Buffered Saline; RA: retinoic acid; TSS: transcription start site; UTR: untranslated region.

Authors' contributions

X.W., J.D., L.Y. and H.-F.D. performed experiments with the assistance of H.C. and L.M. in establishing and characterizing inducible HOXC9 expression cells, L.M. in microarray sample preparation, B.J. and M.R. in ChIP, E.J.L. in ChIP-seq library preparation, and L.C.N. in mass spectrometry. J.-H.C. Y.Z., and H.-F.D. performed microarray and ChIP-seq data analyses. X.W., J.D., H.C., and H.-F.D. designed the study with the assistance of H.S., J.C., and S.H. H.-F.D. wrote the manuscript with contributions from J.D., J.-H.C., L.C.N. and E.J.L. All authors commented on the manuscript.

Acknowledgements

We thank Drs. LesleyAnn Hawthorn and Sam Chang at the Georgia Regents University Cancer Center Genomics Core for assistance in Microarray and ChIP-seq. This work was supported by grants from the National Institutes of Health (CA124982) and Department of Defense (W81XWH-12-1-0613) to H.-F.D., the National Basic Research Program of China (No. 2012cb114603) to H.C., and the National Natural Science

Foundation of China (No. 81172443) to X.W. H.-F.D., H.S., and J.C. are Georgia Cancer Coalition Distinguished Scholars.

References

1. Nouspikel T, Hanawalt PC: **DNA repair in terminally differentiated cells.** *DNA Repair (Amst)* 2002, **1:**59-75.
2. Simonatto M, Latella L, Puri PL: **DNA damage and cellular differentiation: more questions than responses.** *J Cell Physiol* 2007, **213:**642-648.
3. Fortini P, Dogliotti E: **Mechanisms of dealing with DNA damage in terminally differentiated cells.** *Mutat Res* 2010, **685:**38-44.
4. Reya T, Morrison SJ, Clarke MF, Weissman IL: **Stem cells, cancer, and cancer stem cells.** *Nature* 2001, **414:**105-111.
5. Clarke MF, Dick JE, Dirks PB, Eaves CJ, Jamieson CH, Jones DL, Visvader J, Weissman IL, Wahl GM: **Cancer Stem Cells--Perspectives on Current Status and Future Directions: AACR Workshop on Cancer Stem Cells.** *Cancer Res* 2006, **66:**9339-9344.
6. Visvader JE, Lindeman GJ: **Cancer stem cells in solid tumours: accumulating evidence and unresolved questions.** *Nat Rev Cancer* 2008, **8:**755-768.
7. Bao S, Wu Q, McLendon RE, Hao Y, Shi Q, Hjelmeland AB, Dewhirst MW, Bigner DD, Rich JN: **Glioma stem cells promote radioresistance by**

preferential activation of the DNA damage response. *Nature* 2006, **444:**756-760.

8. Phillips TM, McBride WH, Pajonk F: **The response of CD24(-/low)/CD44+ breast cancer-initiating cells to radiation.** *J Natl Cancer Inst* 2006, **98:**1777-1785.

9. Eramo A, Ricci-Vitiani L, Zeuner A, Pallini R, Lotti F, Sette G, Pilozzi E, Larocca LM, Peschle C, De Maria R: **Chemotherapy resistance of glioblastoma stem cells.** *Cell Death Differ* 2006, **13:**1238-1241.

10. Liu G, Yuan X, Zeng Z, Tunici P, Ng H, Abdulkadir IR, Lu L, Irvin D, Black KL, Yu JS: **Analysis of gene expression and chemoresistance of CD133+ cancer stem cells in glioblastoma.** *Mol Cancer* 2006, **5:**67.

11. Brodeur GM: **Neuroblastoma: biological insights into a clinical enigma.** *Nat Rev Cancer* 2003, **3:**203-216.

12. Maris JM: **Recent Advances in Neuroblastoma.** *N Engl J Med* 2010, **362:**2202-2211.

13. Seeds NW, Gilman AG, Amano T, Nirenberg MW: **Regulation of axon formation by clonal lines of a neural tumor.** *Proc Natl Acad Sci U S A* 1970, **66:**160-167.

14. Jensen L, Linn S: **A reduced rate of bulky DNA adduct removal is coincident with differentiation of human neuroblastoma cells induced by nerve growth factor.** *Mol Cell Biol* 1988, **8:**3964-3968.

15. Sidell N: **Retinoic acid-induced growth inhibition and morphologic differentiation of human neuroblastoma cells in vitro.** *J Natl Cancer Inst* 1982, **68:**589-596.

16. Byfield JE, Lee YC, Klisak I, Finklestein JZ: **Effect of differentiation on the repair of DNA single strand breaks in neuroblastoma cells.** *Biochem Biophys Res Commun* 1975, **63:**730-735.

17. McCombe P, Lavin M, Kidson C: **Control of DNA Repair Linked to Neuroblastoma Differentiation.** *Int J Radiat Biol* 1976, **29:**523-531.

18. Lavin MF, McCombe P, Kidson C: **DNA Replication and Post-replication Repair in U.V.-sensitive Mouse Neuroblastoma Cells.** *Int J Radiat Biol* 1976, **30:**31-40.

19. James M, Mansbridge J, Kidson C: **Ultraviolet Radiation Sensitivity of Proliferating and Differentiated Human Neuroblastoma Cells.** *Int J Radiat Biol* 1982, **41:**547-556.

20. Alexander T, Nolte C, Krumlauf R: **Hox genes and segmentation of the hindbrain and axial skeleton.** *Annu Rev Cell Dev Biol* 2009, **25:**431-456.

21. Maden M: **Retinoic acid in the development, regeneration and maintenance of the nervous system.** *Nat Rev Neurosci* 2007, **8:**755-765.

22. Abemayor E, Sidell N: **Human neuroblastoma cell lines as models for the in vitro study of neoplastic and neuronal cell differentiation.** *Environ Health Perspect* 1989, **80:**3-15.

23. Mao L, Ding J, Zha Y, Yang L, McCarthy BA, King W, Cui H, Ding HF: **HOXC9 Links Cell-Cycle Exit and Neuronal Differentiation and Is a Prognostic Marker in Neuroblastoma.** *Cancer Res* 2011, **71:**4314-4324.

24. Zha Y, Ding E, Yang L, Mao L, Wang X, McCarthy BA, Huang S, Ding HF: **Functional dissection of HOXD cluster genes in regulation of neuroblastoma cell proliferation and differentiation.** *PLoS One* 2012, **7:**e40728.

25. Pearson JC, Lemons D, McGinnis W: **Modulating Hox gene functions during animal body patterning.** *Nat Rev Genet* 2005, **6:**893-904.

26. Moens CB, Selleri L: **Hox cofactors in vertebrate development.** *Dev Biol* 2006, **291:**193-206.

27. Shah N, Sukumar S: **The Hox genes and their roles in oncogenesis.** *Nat Rev Cancer* 2010, **10:**361-371.

28. Duester G: **Retinoic acid synthesis and signaling during early organogenesis.** *Cell* 2008, **134:**921-931.

29. Dennis G, Jr., Sherman BT, Hosack DA, Yang J, Gao W, Lane HC, Lempicki RA: **DAVID: Database for Annotation, Visualization, and Integrated Discovery.** *Genome Biol* 2003, **4:**P3.

30. Huang DW, Sherman BT, Lempicki RA: **Systematic and integrative analysis of large gene lists using DAVID bioinformatics resources.** *Nat Protocols* 2008, **4:**44-57.

31. Francis NJ, Landis SC: **Cellular and molecular determinants of sympathetic neuron development.** *Annu Rev Neurosci* 1999, **22:**541-566.

32. Goridis C, Rohrer H: **Specification of catecholaminergic and serotonergic neurons.** *Nat Rev Neurosci* 2002, **3:**531-541.

33. Ernsberger U: **The role of GDNF family ligand signalling in the differentiation of sympathetic and dorsal root ganglion neurons.** *Cell Tissue Res* 2008, **333:**353-371.

34. Rajasekharan S, Kennedy T: **The netrin protein family.** *Genome Biol* 2009, **10:**239.

35. Bell SP, Dutta A: **DNA REPLICATION IN EUKARYOTIC CELLS.** *Annu Rev Biochem* 2002, **71:**333-374.

36. Carmena M, Wheelock M, Funabiki H, Earnshaw WC: **The chromosomal passenger complex (CPC): from easy rider to the godfather of mitosis.** *Nat Rev Mol Cell Biol* 2012, **13:**789-803.

37. Kee Y, D'Andrea AD: **Expanded roles of the Fanconi anemia pathway in preserving genomic stability.** *Genes Dev* 2010, **24:**1680-1694.

38. Liu Y, Kao H-I, Bambara RA: **FLAP ENDONUCLEASE 1: A Central Component of DNA Metabolism.** *Annu Rev Biochem* 2004, **73:**589-615.

39. Trimarchi JM, Lees JA: **Sibling rivalry in the E2F family.** *Nat Rev Mol Cell Biol* 2002, **3:**11-20.

40. Xu X, Bieda M, Jin VX, Rabinovich A, Oberley MJ, Green R, Farnham PJ: **A comprehensive ChIP-chip analysis of E2F1, E2F4, and E2F6 in normal and tumor cells reveals interchangeable roles of E2F family members.** *Genome Res* 2007, **17:**1550-1561.

41. Edlund T, Jessell TM: **Progression from extrinsic to intrinsic signaling in cell fate specification: a view from the nervous system.** *Cell* 1999, **96:**211-224.

42. Ohnuma S, Harris WA: **Neurogenesis and the cell cycle.** *Neuron* 2003, **40:**199-208.

43. Galderisi U, Jori FP, Giordano A: **Cell cycle regulation and neural differentiation.** *Oncogene* 2003, **22:**5208-5219.

44. Salomoni P, Calegari F: **Cell cycle control of mammalian neural stem cells: putting a speed limit on G1.** *Trends Cell Biol* 2010, **20:**233-243.

45. Sherr CJ, Roberts JM: **CDK inhibitors: positive and negative regulators of G1-phase progression.** *Genes Dev* 1999, **13:**1501-1512.

46. Ohnuma S, Philpott A, Wang K, Holt CE, Harris WA: **p27Xic1, a Cdk inhibitor, promotes the determination of glial cells in Xenopus retina.** *Cell* 1999, **99:**499-510.

47. Nguyen L, Besson A, Heng JI, Schuurmans C, Teboul L, Parras C, Philpott A, Roberts JM, Guillemot F: **p27kip1 independently promotes neuronal differentiation and migration in the cerebral cortex.** *Genes Dev* 2006, **20:**1511-1524.

48. Nieto M, Schuurmans C, Britz O, Guillemot F: **Neural bHLH Genes Control the Neuronal versus Glial Fate Decision in Cortical Progenitors.** *Neuron* 2001, **29:**401-413.

49. Sukhanova MJ, Deb DK, Gordon GM, Matakatsu MT, Du W: **Proneural Basic Helix-Loop-Helix Proteins and Epidermal Growth Factor Receptor Signaling**

Coordinately Regulate Cell Type Specification and cdk Inhibitor Expression during Development. *Mol Cell Biol* 2007, **27:**2987-2996.

50. Morkel M, Wenkel J, Bannister AJ, Kouzarides T, Hagemeier C: **An E2F-like repressor of transcription.** *Nature* 1997, **390:**567-568.

51. Gaubatz S, Wood JG, Livingston DM: **Unusual proliferation arrest and transcriptional control properties of a newly discovered E2F family member, E2F-6.** *Proc Natl Acad Sci U S A* 1998, **95:**9190-9195.

52. Cartwright P, Muller H, Wagener C, Holm K, Helin K: **E2F-6: a novel member of the E2F family is an inhibitor of E2F-dependent transcription.** *Oncogene* 1998, **17:**611-623.

53. Trimarchi JM, Fairchild B, Verona R, Moberg K, Andon N, Lees JA: **E2F-6, a member of the E2F family that can behave as a transcriptional repressor.** *Proc Natl Acad Sci U S A* 1998, **95:**2850-2855.

54. Giangrande PH, Zhu W, Schlisio S, Sun X, Mori S, Gaubatz S, Nevins JR: **A role for E2F6 in distinguishing G1/S- and G2/M-specific transcription.** *Genes Dev* 2004, **18:**2941-2951.

55. Velasco G, Hube F, Rollin J, Neuillet D, Philippe C, Bouzinba-Segard H, Galvani A, Viegas-Pequignot E, Francastel C: **Dnmt3b recruitment through E2F6 transcriptional repressor mediates germ-line gene silencing in murine somatic tissues.** *Proc Natl Acad Sci U S A* 2010, **107:**9281-9286.

56. Ogawa H, Ishiguro K, Gaubatz S, Livingston DM, Nakatani Y: **A complex with chromatin modifiers that occupies E2F- and Myc-responsive genes in G0 cells.** *Science* 2002, **296:**1132-1136.

57. Attwooll C, Oddi S, Cartwright P, Prosperini E, Agger K, Steensgaard P, Wagener C, Sardet C, Moroni MC, Helin K: **A novel repressive E2F6 complex containing the polycomb group protein, EPC1, that interacts with EZH2 in a proliferation-specific manner.** *J Biol Chem* 2005, **280:**1199-1208.

58. Deshpande AM, Akunowicz JD, Reveles XT, Patel BB, Saria EA, Gorlick RG, Naylor SL, Leach RJ, Hansen MF: **PHC3, a component of the hPRC-H complex, associates with E2F6 during G0 and is lost in osteosarcoma tumors.** *Oncogene* 2007, **26:**1714-1722.

59. Trojer P, Cao AR, Gao Z, Li Y, Zhang J, Xu X, Li G, Losson R, Erdjument-Bromage H, Tempst P, et al: **L3MBTL2 protein acts in concert with PcG protein-mediated monoubiquitination of H2A to establish a repressive chromatin structure.** *Mol Cell* 2011, **42:**438-450.

60. Nouspikel T, Hanawalt PC: **Impaired nucleotide excision repair upon macrophage differentiation is corrected by E1 ubiquitin-activating enzyme.** *Proc Natl Acad Sci U S A* 2006, **103:**16188-16193.

61. Subramanian A, Tamayo P, Mootha VK, Mukherjee S, Ebert BL, Gillette MA, Paulovich A, Pomeroy SL, Golub TR, Lander ES, Mesirov JP: **Gene set enrichment analysis: a knowledge-based approach for interpreting genome-wide expression profiles.** *Proc Natl Acad Sci U S A* 2005, **102:**15545-15550.

62. Lee TI, Johnstone SE, Young RA: **Chromatin immunoprecipitation and microarray-based analysis of protein location.** *Nat Protocols* 2006, **1:**729-748.

63. Zhang Y, Liu T, Meyer CA, Eeckhoute J, Johnson DS, Bernstein BE, Nusbaum C, Myers RM, Brown M, Li W, Liu XS: **Model-based analysis of ChIP-Seq (MACS).** *Genome Biol* 2008, **9:**R137.

64. Dignam JD, Lebovitz RM, Roeder RG: **Accurate transcription initiation by RNA polymerase II in a soluble extract from isolated mammalian nuclei.** *Nucleic Acids Res* 1983, **11:**1475-1489.

65. Keller A, Nesvizhskii AI, Kolker E, Aebersold R: **Empirical statistical model to estimate the accuracy of peptide identifications made by MS/MS and database search.** *Anal Chem* 2002, **74:**5383-5392.

66. Nesvizhskii AI, Keller A, Kolker E, Aebersold R: **A statistical model for identifying proteins by tandem mass spectrometry.** *Anal Chem* 2003, **75:**4646-4658.

Figure Legends

Figure 1 Global upregulation of neuronal genes by HOXC9. (**A**) Schematic of experiment. Doxy, doxycycline. (**B**) DAVID analysis of upregulated HOXC9-responsive genes for enriched GO biological process categories (enrichment fold > 2.0; FDR <1%). The number of genes for each biological process category is indicated. (**C**) GSEA showing significant enrichment of gene sets involved in synapse organization and biogenesis and neuron differentiation among the genes upregulated by HOXC9. (**D**) Heatmap of select neuronal genes activated by HOXC9.

Figure 2 Global downregulation of cell cycle and DNA repair genes by HOXC9. (**A**) DAVID analysis of downregulated HOXC9-responsive genes for enriched GO biological process categories (enrichment fold > 2.0; FDR <1%). The number of genes for each biological process category is indicated. (**B**) GSEA showing significant enrichment of gene sets involved in mitotic cell cycle, DNA replication and DNA repair among the genes downregulated by HOXC9.

Figure 3 ChIP-seq analysis of HOXC9 genomic distribution. (**A**) Summary of HOXC9-binding peaks and genes identified by ChIP-seq. (**B-C**) Scatter plot analysis (**B**) and ChIP-seq tag profiles of chromosome 21 (**C**) showing a high correlation between two independent HOXC9 ChIP-seq samples. (**D**) Pie chart showing genomic distribution of HOXC9-binding peaks relative to RefSeq functional categories including promoters (within 5 kb upstream of TSS), 5’ UTRs, exons, introns, 3’ UTRs, downstream (within 5

kb downstream of the gene), and intergenic regions (outside -5 ~ +5 kb of genes). (**E**) Histogram showing the distribution of HOXC9-binding peaks relative to the nearest TSS. Peaks were combined in 100 bp. (**F**) Web logo showing the top enriched motif present in HOXC9 ChIP-seq peaks, which corresponds to the binding site for Abd-B, the *Drosophila* ortholog of mammalian HOX9-13 paralogs.

Figure 4 HOXC9 directly induces a large number of neuronal genes. (**A**) DAVID analysis of upregulated HOXC9 target genes for enriched GO biological process categories (enrichment fold > 2.0; FDR < 5%). The number of genes for each biological process category is indicated. (**B**) ChIP-seq tag profiles showing HOXC9 binding to representative upregulated HOXC9 target genes involved in nervous system development (*GFRA3*, top; *RET*, middle; *NTN3*, bottom).

Figure 5 HOXC9 directly represses a large number of cell cycle and DNA repair genes. (**A**) DAVID analysis of downregulated HOXC9 target genes for enriched GO biological process categories (enrichment fold > 2.0; FDR <1%). The number of genes for each biological process category is indicated. (**B-D**) ChIP-seq tag profiles showing HOXC9 binding to representative downregulated HOXC9 target genes involved in DNA replication (**B**), mitosis (**C**), and DNA repair (**D**).

Figure 6 HOXC9 interacts with E2F6 and recruits it to cell cycle genes. (**A**) Reciprocal Co-IP of myc-HOXC9 and E2F6 in nuclear extracts from BE(2)-C/Tet-Off/myc-HOXC9 cells cultured in the absence of doxycycline (Doxy) for 6 days. (**B**)

Size-exclusion chromatography analysis of complexes containing myc-HOXC9, E2F6 or MEIS2 in nuclear extracts of BE(2)-C/Tet-Off/myc-HOXC9 cells cultured in the absence of Doxy for 6 days. (**C**) Co-IP of myc-HOXC9 and E2F6 in pooled Superose-6 fractions 19-21. (**D**) ChIP-qPCR analysis showing E2F6 binding to specific promoter regions of the cell cycle genes *CCNB1* and *CDCA8* in BE(2)-C/Tet-Off/myc-HOXC9 cells before (Doxy+) and after (Doxy-) HOXC9 induction. Dashed lines indicate IgG control. Error bars represent SD (n = 3). Data were analyzed with unpaired, two-tailed Student's *t*-test and *p* values are indicated.

Figure 7 E2F6 is essential for HOXC9 induction of G1 arrest and repression of cell cycle genes. (**A**) Immunoblot analysis of E2F6 levels in BE(2)-C/Tet-Off/myc-HOXC9 cells infected with lentiviruses expressing shRNA against *GFP* or various coding regions of *E2F6*. E2F6 levels were quantified against β-actin. (**B-D**) Phase contrast imaging and growth assay (**B**) and cell cycle analysis (**C, D**) showing E2F6 knockdown abrogated HOXC9-induced growth arrest. Error bars, SD (n = 4). (**E-F**) Immunoblot analysis (**E**) and quantification (**F**) showing that E2F6 knockdown abrogated HOXC9 repression of cyclins, but not HOXC9 induction of NEFM. HOXC9, CCNA2, CCNB1 and NEFM levels were quantified against β-actin with the protein levels in GFPsh-expressing cells cultured in the presence of doxycycline (Doxy+) were defined as 1.0 (dashed lines). Error bars, SD (n = 3). Data in (**D**) and (**F**) were analyzed with unpaired, two-tailed Student's *t*-test and *p* values are indicated.

Figure 10 HOXC9 directly regulates the expression of distinct sets of genes to coordinate diverse cellular events associated with neuronal differentiation.

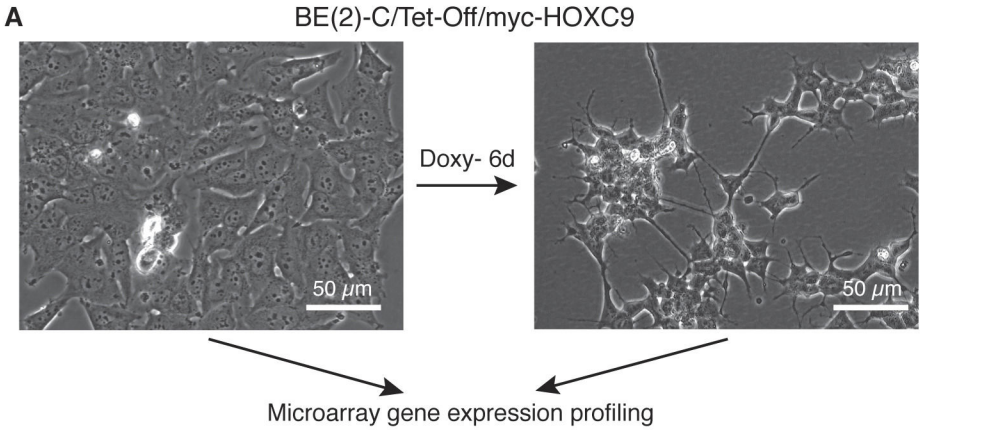
A
BE(2)-C/Tet-Off/myc-HOXC9
Doxy- 6d
50 μm
50 μm
Microarray gene expression profiling

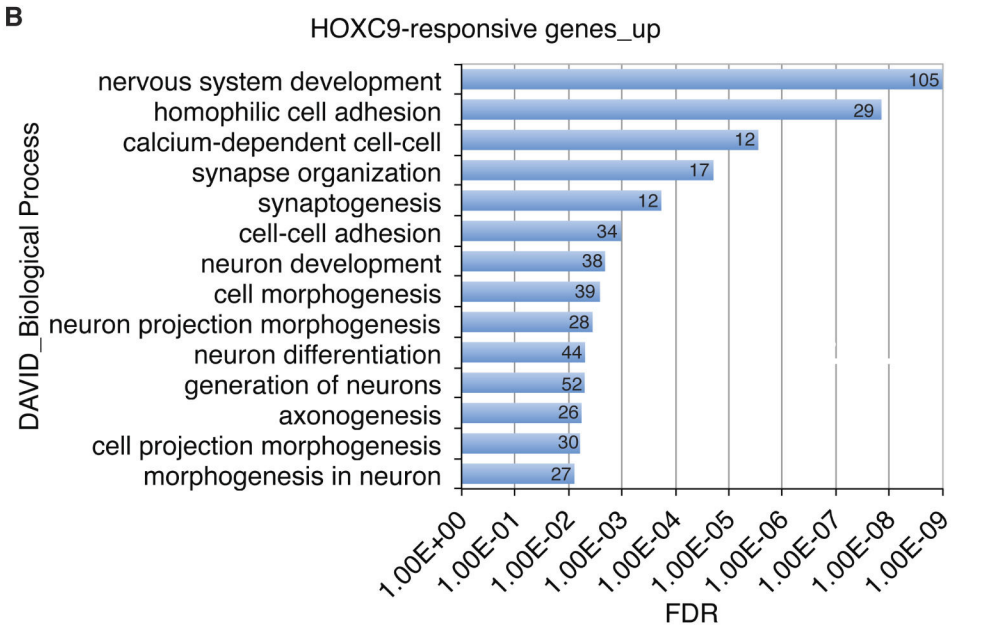
B
HOXC9-responsive genes_up
DAVID_Biological Process
nervous system development 105
homophilic cell adhesion 29
calcium-dependent cell-cell 12
synapse organization 17
synaptogenesis 12
cell-cell adhesion 34
neuron development 38
cell morphogenesis 39
neuron projection morphogenesis 28
neuron differentiation 44
generation of neurons 52
axonogenesis 26
cell projection morphogenesis 30
morphogenesis in neuron 27
1.00E+00
1.00E-01
1.00E-02
1.00E-03
1.00E-04
1.00E-05
1.00E-06
1.00E-07
1.00E-08
1.00E-09
FDR

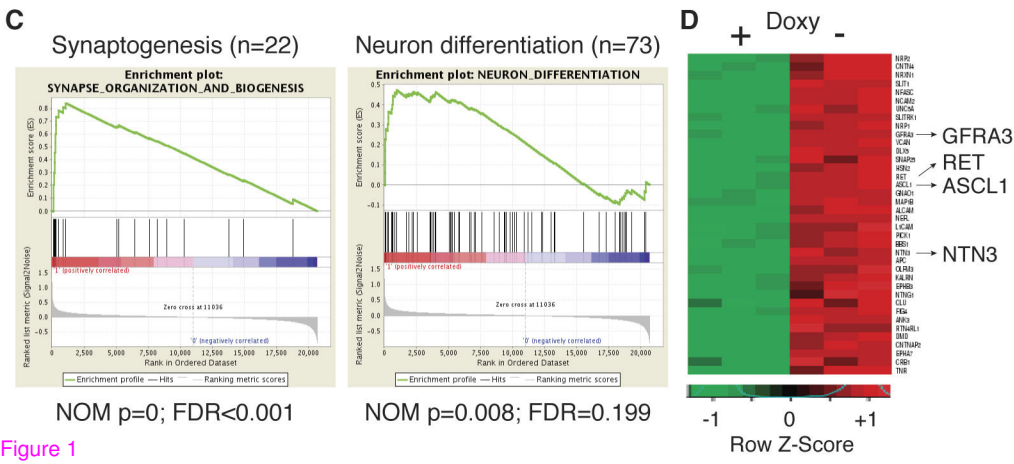
C
Synaptogenesis (n=22)
Enrichment plot: SYNAPSE_ORGANIZATION_AND_BIOGENESIS
Enrichment score (ES)
Ranked list metric (Signal2Noise)
Zero cross at 11036
Rank in Ordered Dataset
Enrichment profile
Hits
Ranking metric scores
NOM p=0; FDR<0.001
Neuron differentiation (n=73)
Enrichment plot: NEURON_DIFFERENTIATION
Zero cross at 11036
Rank in Ordered Dataset
Enrichment profile
Hits
Ranking metric scores
NOM p=0.008; FDR=0.199
D
Doxy
+
-
GFRA3
RET
ASCL1
NTN3
-1
0
+1
Row Z-Score

Figure 1

A

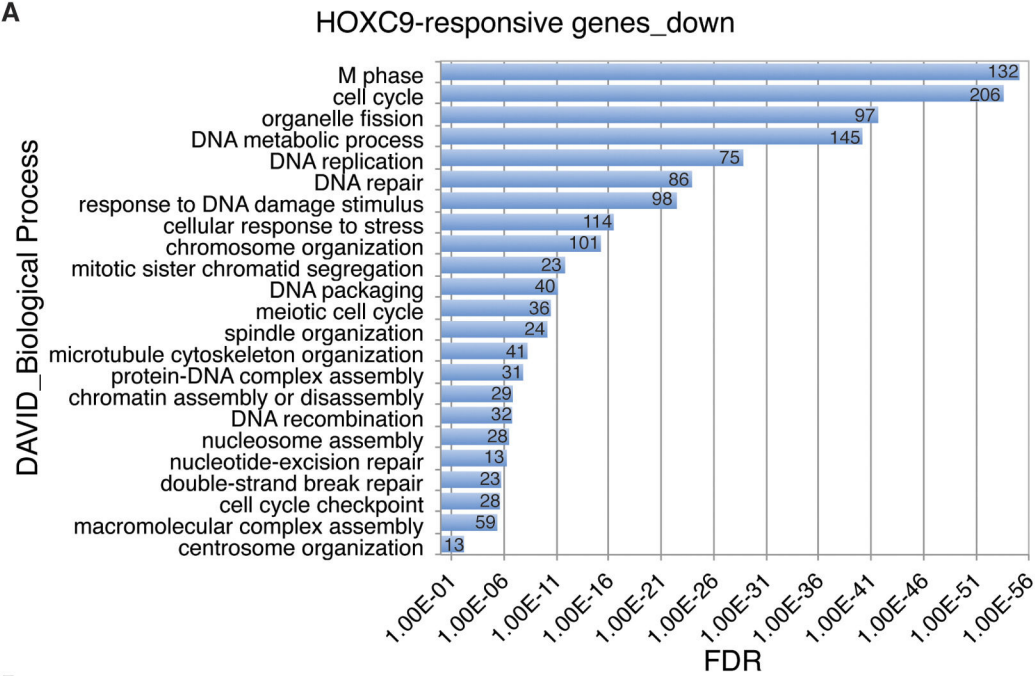

B

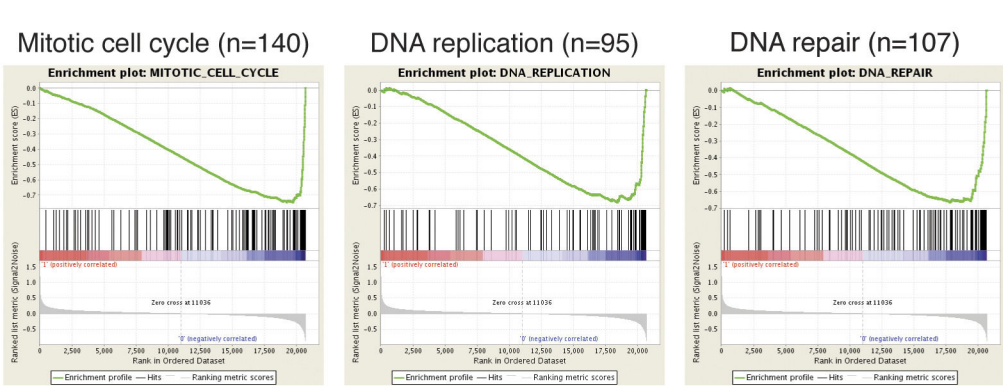

NOM p=0; FDR=0

NOM p=0; FDR=0

NOM p=0; FDR=0

Figure 2

A

Total Reads (10^6)	
Input	41.5
HOXC9	88.3
Peaks (FDR < 1%)	29,221
Genes (within 5 kb of a peak)	4,992

B

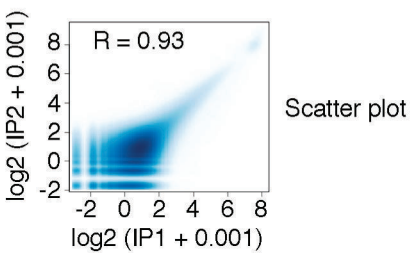

Scatter plot

C

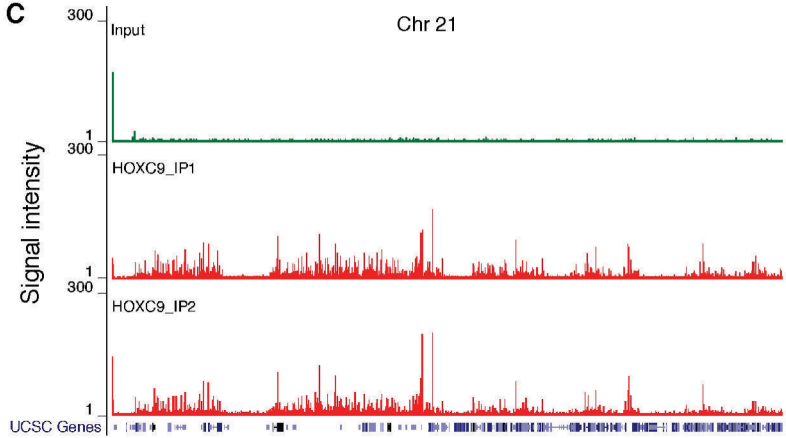

D

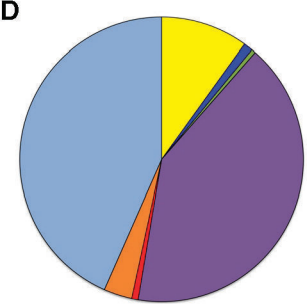

- Promoter (10.0%)
- 5' UTR (1.0%)
- Exon (0.5%)
- Intron (41.2%)
- 3' UTR (0.7%)
- Downstream (3.2%)
- Intergenic (43.4%)

E

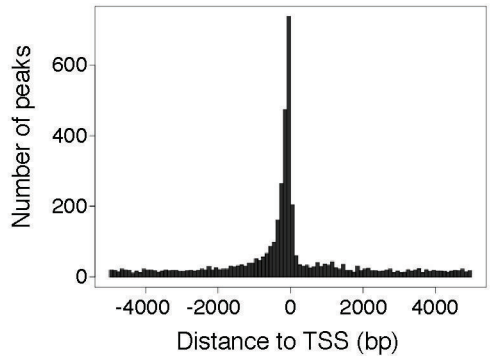

F

E value: 1.6×10^{-35}

Factor: Abd-B

Figure 3

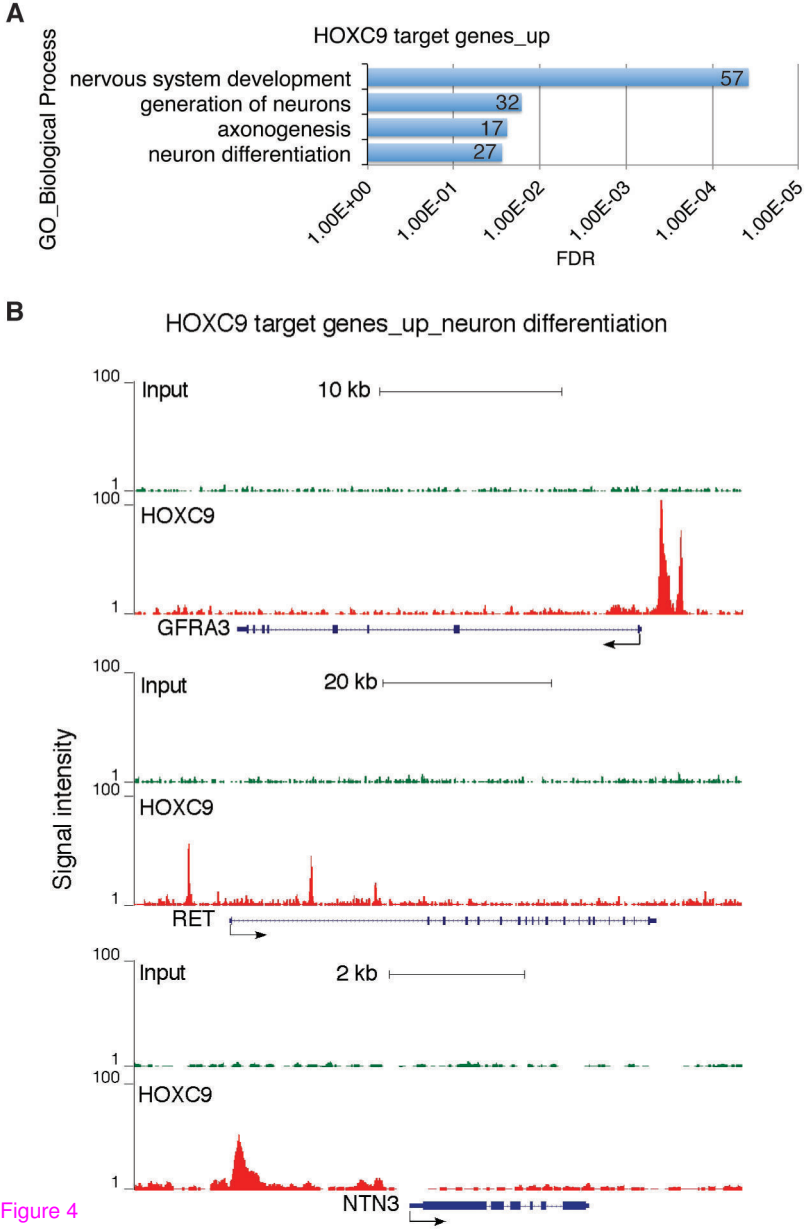
A
HOXC9 target genes_up
GO_Biological Process
nervous system development
generation of neurons
axonogenesis
neuron differentiation
57
32
17
27
1.00E+00
1.00E-01
1.00E-02
1.00E-03
1.00E-04
1.00E-05
FDR
B
HOXC9 target genes_up_neuron differentiation
Signal intensity
Input
10 kb
HOXC9
GFRA3
Input
20 kb
HOXC9
RET
Input
2 kb
HOXC9
NTN3
100
1

Figure 4

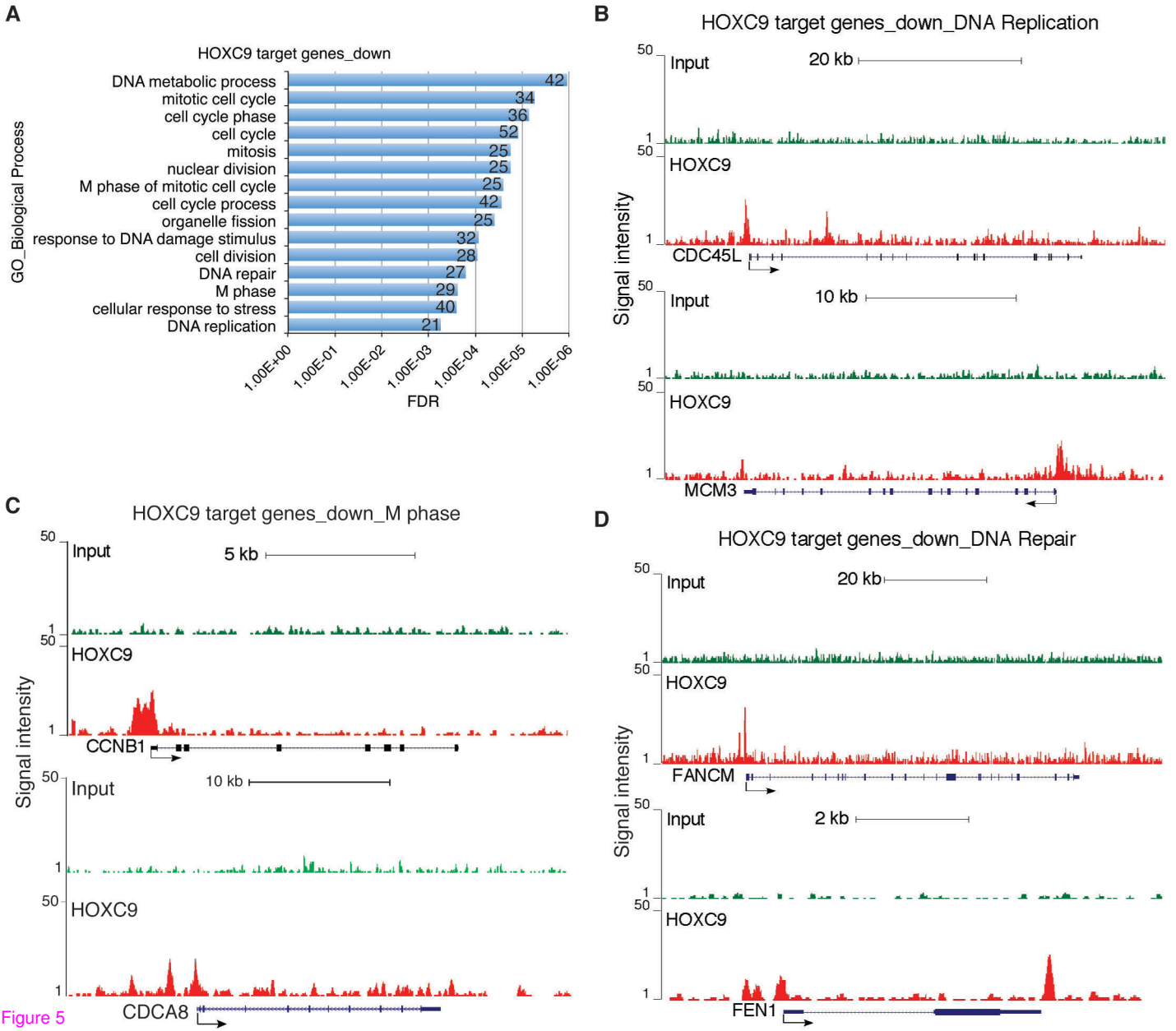
A
HOXC9 target genes_down
GO_Biological Process
DNA metabolic process 42
mitotic cell cycle 34
cell cycle phase 36
cell cycle 52
mitosis 25
nuclear division 25
M phase of mitotic cell cycle 25
cell cycle process 42
organelle fission 25
response to DNA damage stimulus 32
cell division 28
DNA repair 27
M phase 29
cellular response to stress 40
DNA replication 21
1.00E+00
1.00E-01
1.00E-02
1.00E-03
1.00E-04
1.00E-05
1.00E-06
FDR
B
HOXC9 target genes_down_DNA Replication
Signal intensity
Input
20 kb
HOXC9
CDC45L
Input
10 kb
HOXC9
MCM3
C
HOXC9 target genes_down_M phase
Signal intensity
Input
5 kb
HOXC9
CCNB1
Input
10 kb
HOXC9
CDCA8
D
HOXC9 target genes_down_DNA Repair
Signal intensity
Input
20 kb
HOXC9
FANCM
Input
2 kb
HOXC9
FEN1

Figure 5

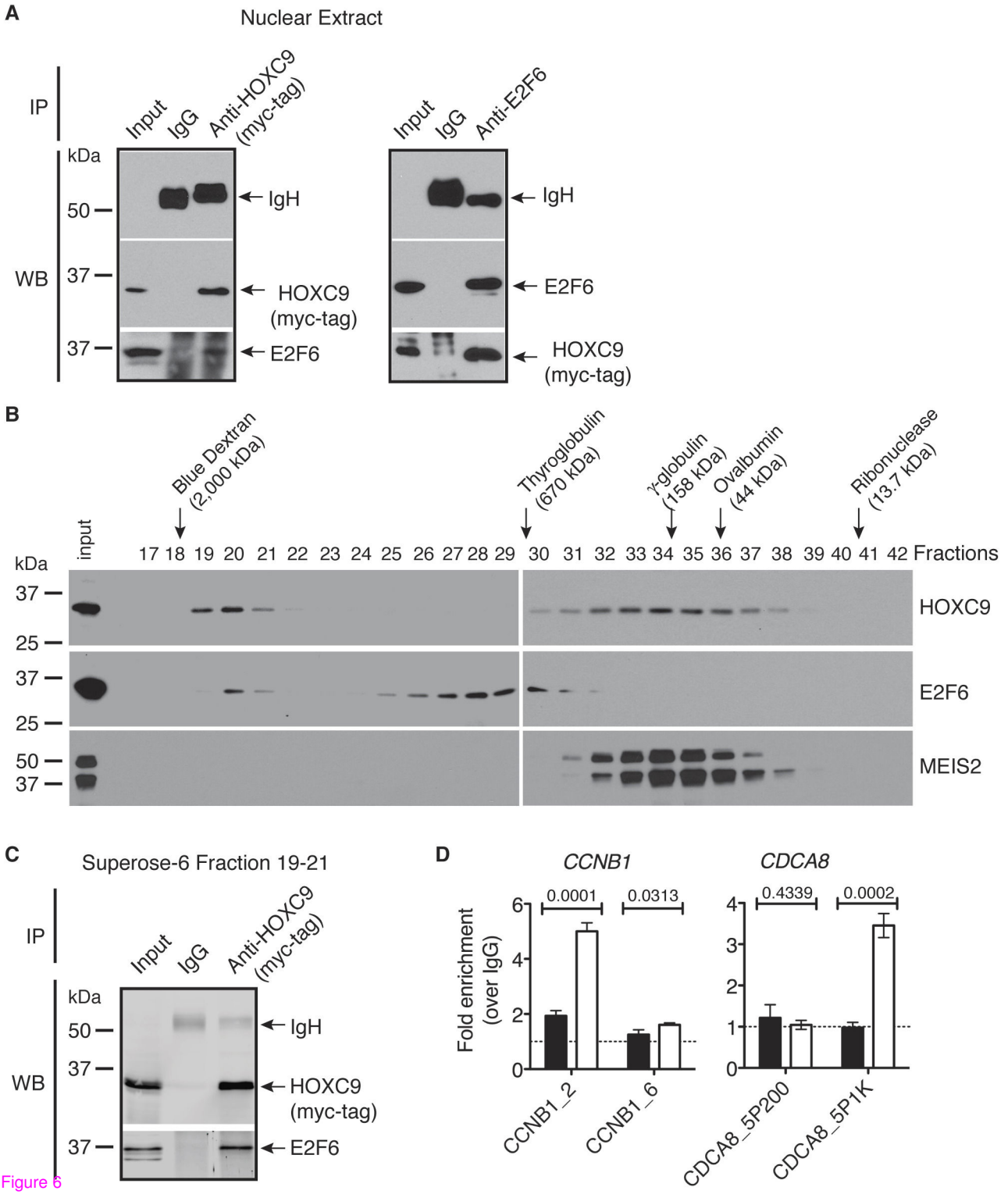
A
Nuclear Extract
IP
Input
IgG
Anti-HOXC9 (myc-tag)
Input
IgG
Anti-E2F6
kDa
50
37
WB
37
IgH
HOXC9 (myc-tag)
E2F6
IgH
E2F6
HOXC9 (myc-tag)
B
Blue Dextran (2,000 kDa)
Thyroglobulin (670 kDa)
γ-globulin (158 kDa)
Ovalbumin (44 kDa)
Ribonuclease (13.7 kDa)
input
17 18 19 20 21 22 23 24 25 26 27 28 29 30 31 32 33 34 35 36 37 38 39 40 41 42 Fractions
kDa
37
25
37
25
50
37
HOXC9
E2F6
MEIS2
C
Superose-6 Fraction 19-21
IP
Input
IgG
Anti-HOXC9 (myc-tag)
kDa
50
37
WB
37
IgH
HOXC9 (myc-tag)
E2F6
D
CCNB1
CDCA8
Fold enrichment (over IgG)
0.0001
0.0313
0.4339
0.0002
6
4
2
0
4
3
2
1
0
CCNB1_2
CCNB1_6
CDCA8_5P200
CDCA8_5P1K

Figure 6

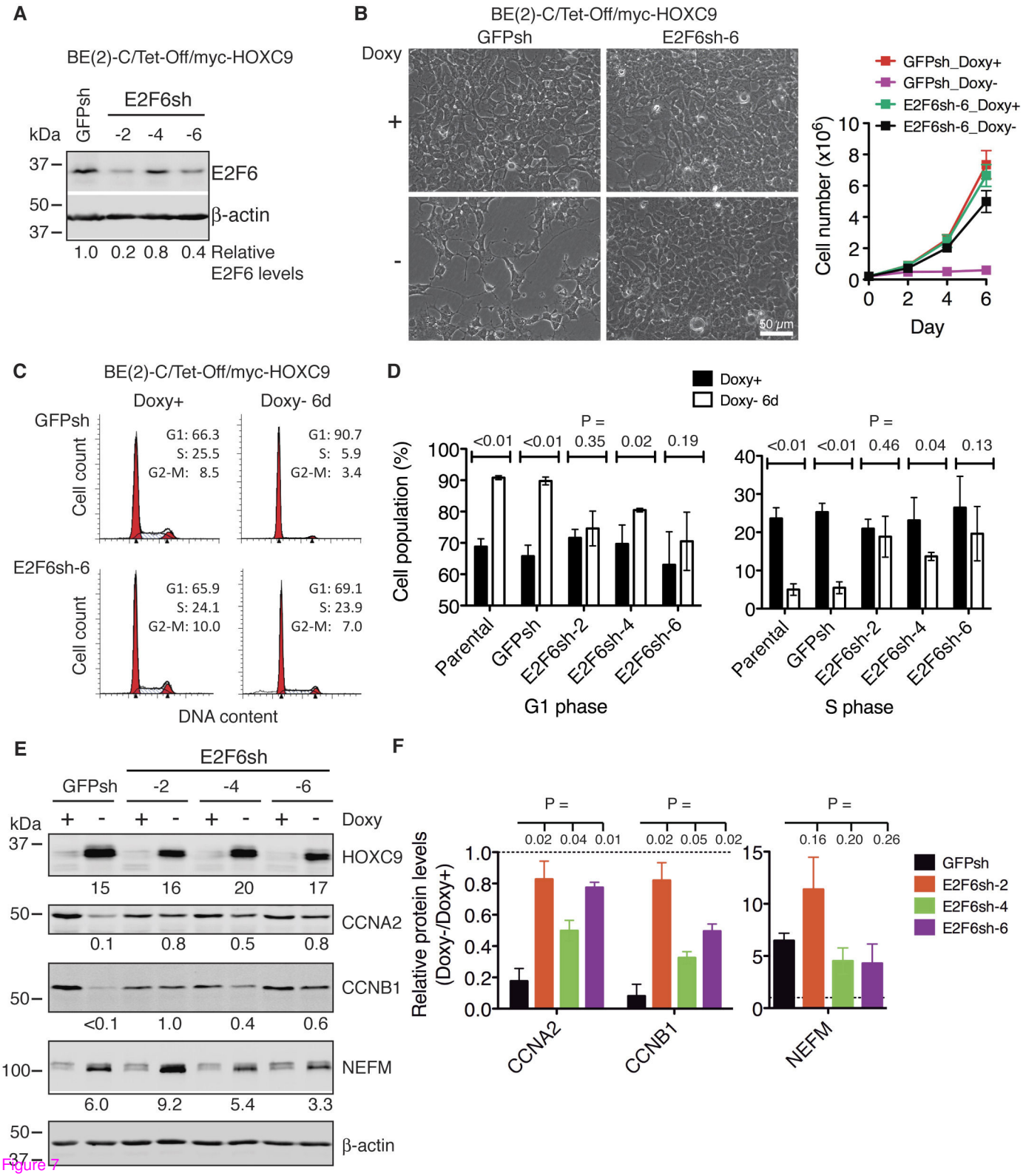
A
BE(2)-C/Tet-Off/myc-HOXC9
GFPsh
E2F6sh
kDa
-2
-4
-6
37
E2F6
50
β-actin
37
1.0 0.2 0.8 0.4 Relative E2F6 levels
B
BE(2)-C/Tet-Off/myc-HOXC9
GFPsh
E2F6sh-6
Doxy
+
-
50 μm
GFPsh_Doxy+
GFPsh_Doxy-
E2F6sh-6_Doxy+
E2F6sh-6_Doxy-
Cell number (x10^6)
Day
C
BE(2)-C/Tet-Off/myc-HOXC9
Doxy+
Doxy- 6d
GFPsh
Cell count
G1: 66.3
S: 25.5
G2-M: 8.5
G1: 90.7
S: 5.9
G2-M: 3.4
E2F6sh-6
G1: 65.9
S: 24.1
G2-M: 10.0
G1: 69.1
S: 23.9
G2-M: 7.0
DNA content
D
Doxy+
Doxy- 6d
Cell population (%)
P =
<0.01 <0.01 0.35 0.02 0.19
<0.01 <0.01 0.46 0.04 0.13
Parental
GFPsh
E2F6sh-2
E2F6sh-4
E2F6sh-6
G1 phase
S phase
E
E2F6sh
GFPsh
-2
-4
-6
kDa
Doxy
HOXC9
15 16 20 17
CCNA2
0.1 0.8 0.5 0.8
CCNB1
<0.1 1.0 0.4 0.6
NEFM
6.0 9.2 5.4 3.3
β-actin
F
P =
0.02 0.04 0.01
0.02 0.05 0.02
0.16 0.20 0.26
Relative protein levels (Doxy-/Doxy+)
CCNA2
CCNB1
NEFM
GFPsh
E2F6sh-2
E2F6sh-4
E2F6sh-6

ding_Fig8

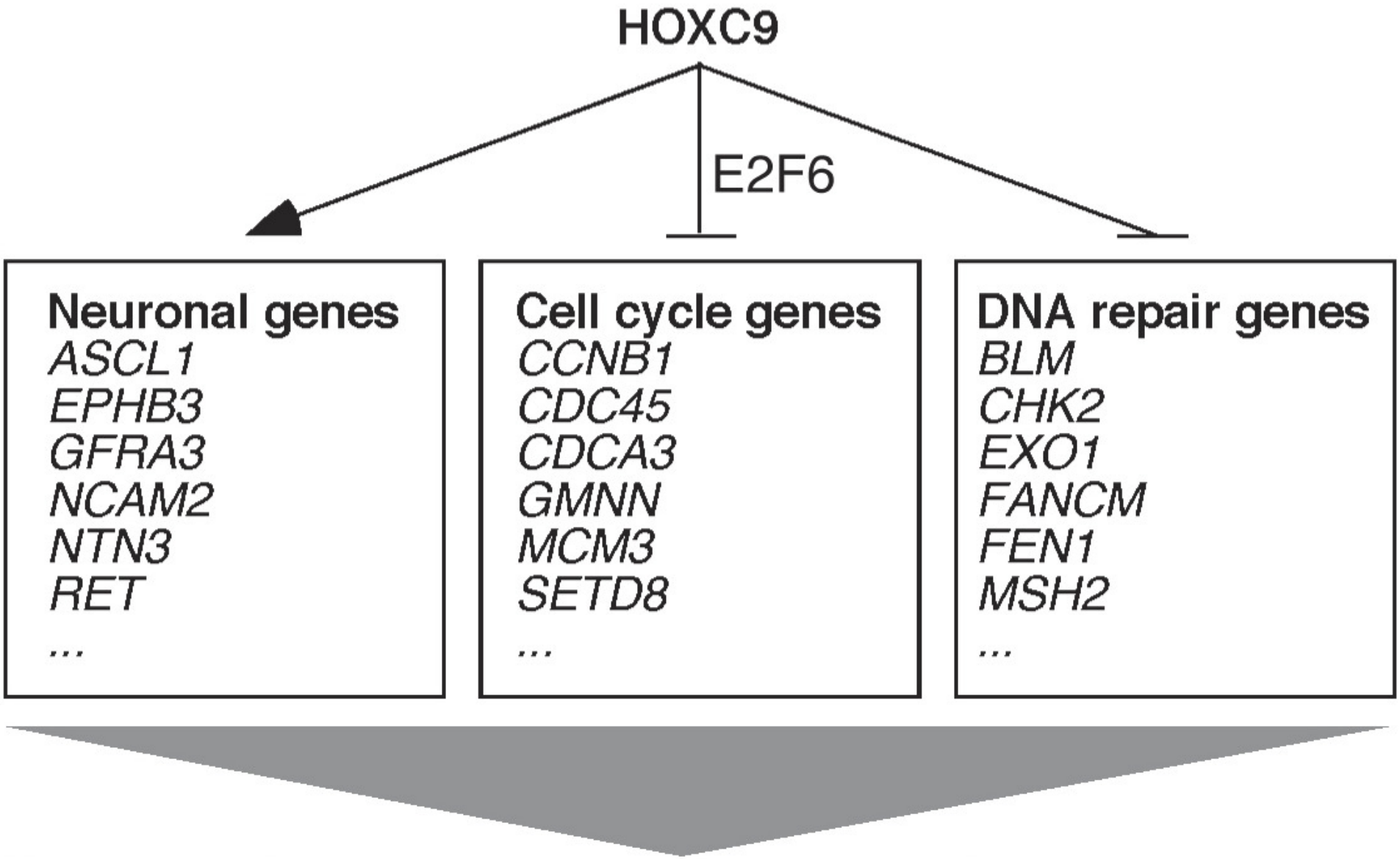

Figure 8

Additional files provided with this submission:

Additional file 1: ding_Add file 1.pdf, 4284K
http://genomebiology.com/imedia/1111857438103195/supp1.pdf
Additional file 2: Table S1_HOXC9 responsive genes.xlsx, 155K
http://genomebiology.com/imedia/1297841751031957/supp2.xlsx
Additional file 3: Table S2_GO HOXC9-responsive genes_up.xlsx, 77K
http://genomebiology.com/imedia/2038952256103195/supp3.xlsx
Additional file 4: Table S3_GO HOXC9-responsive genes_down.xlsx, 115K
http://genomebiology.com/imedia/3452798701031957/supp4.xlsx
Additional file 5: Table S4 HOXC9-binding peaks.xlsx, 1867K
http://genomebiology.com/imedia/7039543031031957/supp5.xlsx
Additional file 6: Table S5 HOXC9-binding genes.xlsx, 500K
http://genomebiology.com/imedia/1402112299103195/supp6.xlsx
Additional file 7: Table S6 HOXC9 target genes.xls, 213K
http://genomebiology.com/imedia/4415724121031957/supp7.xls
Additional file 8: Table S7 GO_HOXC9 direct targets_up.xlsx, 71K
http://genomebiology.com/imedia/5773860561031957/supp8.xlsx
Additional file 9: Table S8 GO_HOXC9 direct targets_down.xls, 77K
http://genomebiology.com/imedia/4200865301031957/supp9.xls